The Polar Express: Optimal Matrix Sign Methods and Their Application to the **Muon** Algorithm

Noah Amsel* David Persson[†] Christopher Musco[‡] Robert M. Gower[§]
September 29, 2025

Abstract

Computing the polar decomposition and the related matrix sign function has been a well-studied problem in numerical analysis for decades. Recently, it has emerged as an important subroutine within the Muon algorithm for training deep neural networks. However, the requirements of this application differ sharply from classical settings: deep learning demands GPU-friendly algorithms that prioritize high throughput over high precision. We introduce Polar Express, a new method for computing the polar decomposition. Like Newton–Schulz and other classical polynomial methods, our approach uses only matrix-matrix multiplications, making it very efficient on GPUs. Inspired by earlier work of Chen & Chow and Nakatsukasa & Freund, Polar Express adapts the update rule at each iteration by solving a minimax optimization problem. We prove that this strategy minimizes error in a worst-case sense, allowing Polar Express to converge as rapidly as possible both in the early iterations and asymptotically. We also address finite-precision issues, making it practical to use in bfloat16. When integrated into the Muon training framework, our method leads to consistent improvements in validation loss when training a GPT-2 model on one billion tokens from the FineWeb dataset, outperforming recent alternatives across a range of learning rates.

1 Introduction

Advanced linear algebra is making its way into deep learning. Efficient algorithms for computing *matrix functions* have found exciting new applications in training neural networks. In particular, approximations to the matrix-inverse are used in the full Adagrad method [15], the matrix square-root and quarter-root appear as subroutines in the Shampoo and Soap optimizers [20, 48, 51], and most recently, the matrix sign function has become a key ingredient of the Muon optimizer [5, 4, 25].

While the problem of computing these matrix functions has been studied by numerical analysts for decades, applications in deep learning come with different requirements than those in computational science. For deep learning, it is critical to take maximum advantage of GPU-friendly operations like matrix-matrix products and to avoid less parallel operations. Moreover, memory overhead must be small to handle large models. On the other hand,

^{*}New York University. noah.amsel@nyu.edu

[†]New York University and Flatiron Institute. dup210@nyu.edu, dpersson@flatironinstitute.org

[‡]New York University. cmusco@nyu.edu

[§]Flatiron Institute. rgower@flatironinstitute.org

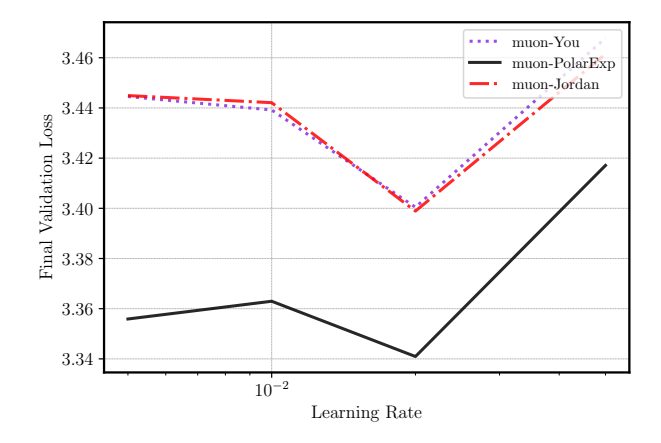
https://github.com/NoahAmsel/PolarExpress

Algorithm 1 Python code for the Polar Express of degree = 5.

```
from itertools import repeat
import torch
coeffs_list = [
    (8.28721201814563, -23.595886519098837, 17.300387312530933),
    (4.107059111542203, -2.9478499167379106, 0.5448431082926601),
    (3.9486908534822946, -2.908902115962949, 0.5518191394370137),
    (3.3184196573706015, -2.488488024314874, 0.51004894012372),
    (2.300652019954817, -1.6689039845747493, 0.4188073119525673),
    (1.891301407787398, -1.2679958271945868, 0.37680408948524835),
    (1.8750014808534479, -1.2500016453999487, 0.3750001645474248),
    (1.875, -1.25, 0.375), # subsequent coeffs equal this numerically
# safety factor for numerical stability (but exclude last polynomial)
coeffs_list = [(a / 1.01, b / 1.01**3, c / 1.01**5)]
                for (a, b, c) in coeffs_list[:-1]] + [coeffs_list[-1]]
@torch.compile
def PolarExpress(G: torch.Tensor, steps: int) -> torch.Tensor:
   assert G.ndim >= 2
   X = G.bfloat16() # for speed
   if G.size(-2) > G.size(-1): X = X.mT # this reduces FLOPs
   X = X / (X.norm(dim=(-2, -1), keepdim=True) * 1.01 +1e-7)
   hs = coeffs_list[:steps] + list(
        repeat(coeffs_list[-1], steps - len(coeffs_list)))
    for a, b, c in hs:
        A = X @ X.mT
        B = b * A + c * A @ A
        X = a * X + B @ X # X < -aX + bX^3 + cX^5
    if G.size(-2) > G.size(-1): X = X.mT
    return X
```

high accuracy is typically less important; the gold standard of sixteen digits of accuracy is overkill in deep learning.

Given these considerations, there is a need to develop new matrix function methods that are tailor-made for deep learning applications. We take on this challenge by designing a state-of-the-art, GPU-friendly algorithm for computing the matrix sign function, or more generally, for computing the *polar decomposition* of a rectangular matrix. We apply our new Polar Express method (Algorithm 1) to compute the descent direction in the increasingly popular Muon optimizer. In Figure 1, we show that using Polar Express within Muon consistently results in lower validation loss across all learning rates when training a GPT-2 model, as compared to other matrix sign methods [10, 36, 25].



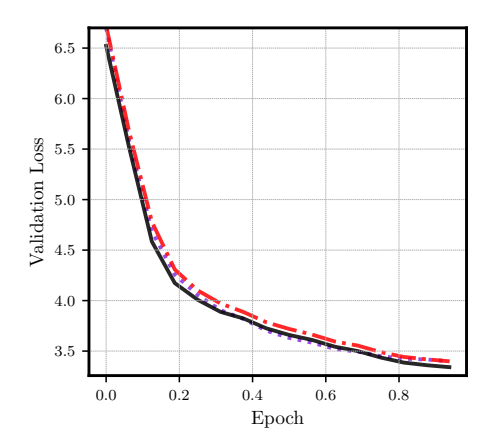


Figure 1: Training a GPT-2-Large model (774M params) on 1 billion tokens from the FineWeb dataset [2]. The label muon-<name> refers to implementing Muon using <name> to compute the polar factor. Left: final validation loss across learning rates. Right: validation loss across epochs using the best learning rate. The best learning rate (lr) and final validation loss for each method was adamw (lr = 0.0001): 4.172, muon-You (lr = 0.02): 3.400, muon-Jordan (lr = 0.02): 3.398 and muon-PolarExp (lr = 0.02): 3.340.

1.1 The Muon Method

The Muon optimizer has recently gained popularity for training large language models, often outperforming state-of-the-art adaptive gradient methods like Adam and AdamW [30, 35]. Muon has been used to set records for the NanoGPT speedrun [25], to expand the Pareto frontier of performance versus training FLOPs for large language models [34, 47], and even to train a 32-billion parameter frontier LLM [29].

The Muon update rule [5] is defined as follows. Let $\lambda, \beta > 0$ be the learning rate and momentum coefficient hyperparameters. (By default, $\beta = 0.9$.) Let $\mathbf{W}_t \in \mathbb{R}^{m \times n}$ be the weight matrix of a given neural network layer at iteration t, and let $\mathbf{G}_t \in \mathbb{R}^{m \times n}$ be its (stochastic) gradient. Let $\mathbf{M}_t \in \mathbb{R}^{m \times n}$ be the running momentum estimate of the gradient, where $\mathbf{M}_0 = \mathbf{0}$. The Muon update is given by

$$M_t = \beta M_{t-1} + (1 - \beta)G_t$$
$$W_{t+1} = W_t - \lambda \operatorname{polar}(M_t).$$

Whereas standard stochastic gradient descent (SGD) with momentum updates the weight matrix by taking a step in the direction $-\mathbf{M}_t$, the Muon method steps in the direction $-\operatorname{polar}(\mathbf{M}_t)$, where $\operatorname{polar}(\mathbf{M})$ denotes the closest semi-orthogonal matrix to \mathbf{M} [22, Chapter 8]. Concretely, if $\mathbf{M} = \mathbf{U} \mathbf{\Sigma} \mathbf{V}^{\mathsf{T}}$ is the singular value decomposition (SVD) of \mathbf{M} , then

$$polar(\mathbf{M}) := \mathbf{U}\mathbf{V}^{\mathsf{T}}.\tag{1}$$

The matrix polar(M) can be seen as a generalization of the matrix sign function to rectangular matrices [3]. Indeed, when M is square symmetric with eigendecomposition $M = V\Lambda V^{\mathsf{T}}$, polar(M) exactly coincides with the matrix sign function $\mathrm{sign}(M) = V \mathrm{sign}(\Lambda) V^{\mathsf{T}}$ [22, Chapter 5]. Equivalently, $\mathrm{polar}(M)$ is the left orthogonal factor of the polar decomposition of M [22, Chapter 8]. The motivation for Muon is that $-\mathrm{polar}(M)$ gives the steepest-descent direction with respect to the *spectral norm* (instead of the Frobenius norm, as in standard SGD).

Recent work [45] shows that Muon can be viewed as a conditional gradient (Frank-Wolfe) method with a trust region defined by the spectral norm. In the same work, the authors also provide a convergence theory for the smooth and non-convex setting, as well as for the stochastic non-convex case. The analysis of Muon was further refined in [46], which proves convergence under a layerwise (L_0, L_1) -smoothness assumption, in both the stochastic non-convex and stochastic Polyak–Łojasiewicz settings. We also note earlier work that anticipated Muon's use of the polar factor and its motivation as steepest descent under the spectral norm [8, 9]. We refer the reader to [25] and [5] for further background. In this paper, we take the Muon update rule as given and focus on the problem of efficiently computing the polar decomposition polar (M).

1.2 Computing the Polar Factor

Although polar(M) can be computed directly via an SVD in $O(\min(mn^2, nm^2))$ time, doing so is prohibitively expensive in deep learning applications, especially as standard SVD algorithms fail to take full advantage of the parallelism available on GPUs. There has been significant work on highly-parallel methods for the SVD, but the most common approaches actually require computing the matrix-sign function as a subroutine [38, 40]. Numerical analysts have spent decades developing iterative methods for computing polar(M). This rich line of work includes Newton–Schulz [22, Chapter 8], Padé iteration [28, 21], the Newton and scaled Newton iterations [22, Chapter 8], the QWHD iteration [37, 40], and Zolo-pd (Zolotarev polar decomposition) [38]. Unfortunately, as discussed in Section 2, most of these methods are based on rational approximations to the function sign(x) and require computing matrix inverses or QR decompositions. Such methods are ill-suited to GPU acceleration and deep learning applications. In contrast, the older Newton-Schulz method is based on polynomial approximation of sign(x) and uses only matrix-matrix products. Thus, Muon initially used Newton-Schulz [4]. Indeed, Muon stands for "MomentUm Orthogonalized by Newton-Schulz" [25].

The Newton-Schulz methods. Newton-Schulz constructs a sequence of approximations $X_t \approx \text{polar}(M)$ as follows:

$$X_0 = M/\|M\|_{\text{F}}$$
 $X_{t+1} = \frac{3}{2}X_t - \frac{1}{2}X_tX_t^{\top}X_t$ (2)

At each iteration, this rule effectively applies the cubic polynomial $p(x) = \frac{3}{2}x - \frac{1}{2}x^3$ to each singular value of X_t . The scalar fixed-point iteration $x_{t+1} = p(x_t)$ converges to $\operatorname{sign}(x_0)$ as $t \to \infty$, provided $|x_0| \le 1$. As a result, the matrix iteration satisfies $\lim_{t \to \infty} X_t = UV^{\top} = \operatorname{polar}(X_0)$. Higher-degree versions of Newton-Schulz follow the same principle. For example, the degree-5 polynomial $p(x) = (15x - 10x^3 + 3x^5)/8$ converges even faster. The Newton-Schulz iterations converge super-exponentially when X_t is sufficiently close to $\operatorname{polar}(M)$, but they suffer from slow initial convergence; when X_0 is far from $\operatorname{polar}(M)$, the approximation improves slowly over the first few iterations.

The Jordan and You methods. In Muon, high accuracy approximations to polar(M) are usually not necessary. The primary goal is instead to compute a coarse approximation in as few iterations as possible. To accelerate convergence in the low-accuracy regime, Jordan recently proposed a fixed-point iteration based on the polynomial p(x) = 3.4445x - 1.000

 $4.7750x^3 + 2.0315x^5$ [25], which was found using a heuristic numerical search. Unlike Newton-Schulz, the scheme that Jordan proposed does not converge to polar(M). Instead, it plateaus at an error of ≈ 0.3 . However, it reaches this level of accuracy rapidly. As a result, when the number of iterations is smaller than about 10, Jordan's method outperforms the Newton-Schulz iteration. Building on this idea, You [10] proposed a method that applies six different polynomial updates in succession, which were again found by heuristic search. This method achieves better accuracy than Jordan's but still fails to converge.

We introduce a new method. In particular, we derive polynomial update rules that are *optimal* at every iteration, outperforming all previous polynomial methods in our setting.

1.3 Contributions

We present Polar Express², an iterative method for approximating polar(M). Our method dynamically adapts the polynomial update rule at each iteration, prioritizing rapid progress in the initial stage and high accuracy in the later stage. Polar Express constructs polynomials p_1, \ldots, p_T so that the resulting composition is the optimal approximation to the sign function with respect to the supremum (L^{∞}) norm (Theorem 4.1). By iteratively applying these polynomials to M, Polar Express computes an approximation to polar(M) that is optimal in the worst-case at every iteration. Our method converges to polar(M) super-exponentially (Theorem 4.3), and it quickly reaches a good approximation within just five to ten iterations. This early-stage acceleration is especially valuable in deep learning applications, where runtime efficiency takes precedence over high accuracy. In contrast, classical methods like Newton-Schulz suffer from a slow initial convergence, while recent heuristic proposals [25, 10] fail to converge. Our method is efficient to run on GPUs, using only a few matrix-matrix products per iteration.³

We give an explicit instantiation of Polar Express in Algorithm 1, which incorporates minor modifications to make it compatible with half-precision arithmetic (see Section 4.4). Algorithm 1 can be used as a drop-in replacement for previous methods. In numerical experiments, Polar Express outperforms previous methods on synthetic matrices and gradient matrices from a GPT-2 transformer (Figure 4). We demonstrate the effectiveness of using Polar Express within the Muon optimizer in Figure 1, showing that it consistently improves the training of GPT-2 language models on 1 billion tokens of the FineWeb dataset [2].

Notation. We let $\|M\|_{F}$ and $\|M\|_{2}$ denote the Frobenius norm and spectral norm (largest singular value) of a matrix M, respectively. We denote the spectrum (set of singular values) by $\sigma(M)$.

Let \mathbb{P}_d be the set of polynomials of degree at most d. For odd d, $\mathbb{P}_d^{\text{odd}}$ denotes the set of polynomials of degree at most d containing only odd-degree monomials. For a polynomial p, $\deg(p)$ is its degree. Let $\operatorname{sign}(x)$ be the scalar sign function, which satisfies $\operatorname{sign}(0) = 0$, $\operatorname{sign}(x) = 1$ if x > 0 and $\operatorname{sign}(x) = -1$ if x < 0.

For a polynomial $p \in \mathbb{P}_d^{\text{odd}}$ and a matrix M with rank reduced SVD given by $M = U\Sigma V^{\mathsf{T}}$ and positive singular values $\sigma_1 \geq \cdots \geq \sigma_{\text{rank}(M)} > 0$, we define $p(M) := Up(\Sigma)V^{\mathsf{T}}$, where $p(\Sigma)$ is the diagonal matrix with diagonal entries $p(\sigma_i)$ for $i = 1, \ldots, \text{rank}(M)$.

²https://github.com/NoahAmsel/PolarExpress

³In Appendices E and F, we describe two further algorithmic ideas that can be incorporated into Polar Express. They are not used in our Muon experiments but they may be beneficial in other settings, and we believe they merit further study.

2 Related Work

Computing polar(M) is an important and longstanding problem in numerical linear algebra, with applications spanning electronic structure calculations, lattice quantum chromodynamics, orthogonal Procrustes analysis, parallel algorithms for computing the SVD, and beyond; see e.g. [21, 26, 14, 18, 41, 49].

Newton-Schulz and polynomial Padé methods. The earliest methods in the literature are polynomial iterations like (2). Several nearly simultaneous papers introduced the family of polynomial Padé iterations, comprising Newton-Schulz and its higher-degree analogues [31, 6, 21, 33]. These higher-degree methods are also sometimes called "Newton-Schulz"; when doing so, we will specify the degree for clarity. In these methods, each iteration refines the current approximation X_t by applying a low-degree odd matrix polynomial, where any odd monomial $x \mapsto x^{2q+1}$ is defined for rectangular matrices by the formula $X_t \mapsto X_t \left(X_t^\top X_t \right)^q$. Our Polar Express method also takes this form, though unlike Newton-Schulz, it changes the polynomial at each iteration.

The polynomials used in Padé methods are chosen to match the value and first few derivatives of $\operatorname{sign}(x)$ at the points $x=\pm 1$. For instance, the update rule of the third method in this family is defined by $p(x)=\frac{1}{16}\left(35x-35x^3+21x^5-5x^7\right)$, which is the unique degree-7 polynomial satisfying $p(\pm 1)=\pm 1$ and $p'(\pm 1)=p''(\pm 1)=p'''(\pm 1)=0$. These methods converge so long as all singular values of X_0 lie in (0,1], a condition guaranteed by the initialization of (2). Furthermore, the order of convergence of the degree 2q+1 method is q+1 [6]. In particular, the Newton-Schulz method (q=1) converges quadratically.

Newton's method and rational Padé. In the numerical analysis literature, polynomial methods were succeeded by rational iterations like Newton's method [21], defined as follows⁴:

$$\boldsymbol{X}_{0} = \boldsymbol{M} \qquad \qquad \boldsymbol{X}_{t+1} = \frac{1}{2} \left(\boldsymbol{X}_{t} + \boldsymbol{X}_{t}^{-\top} \right)$$
 (3)

Newton's method also converges quadratically. Like Newton-Schulz, it works because the rational function $r(x) = \frac{1}{2}(x+x^{-1})$ has a stable fixed point at 1; unlike for Newton-Schulz, this point is a global attractor for the whole positive real line. At first glance, Newton's method has nothing to do with the Padé iterations discussed above. However, after a change of variables $\mathbf{Y}_t = \mathbf{X}_t^{-1}$, it can be reinterpreted as $\mathbf{Y}_{t+1} = 2\mathbf{Y}_t(\mathbf{I} + \mathbf{Y}_t^{\top}\mathbf{Y}_t)^{-1}$, which is sometimes called inverse Newton. Observing that $r(x) = \frac{2x}{1+x^2}$ satisfies $r(\pm 1) = \pm 1$ and $r'(\pm 1) = 0$, we see that (inverse) Newton is also a Padé method, though a rational rather than polynomial one. In fact, given a odd degree $2q_n + 1$ for the numerator and an even degree $2q_d$ for the denominator, there is a unique rational function that matches the value and first $q_n + q_d$ derivatives of $\mathrm{sign}(x)$ at $x = \pm 1$. This directly yields a Padé method for computing $\mathrm{polar}(\mathbf{M})$ whose order of convergence is $q_n + q_d + 1$. For instance, $r(x) = \frac{3x+x^3}{1+3x^2}$ is called Halley's method, which converges cubically. When $q_d = 0$, we recover the polynomial Padé methods.

 $^{^4}$ Our description of Newton's method and other rational methods assumes square non-singular M. Non-square problems can be reduced to the square case by an initial QR decomposition, but this is not an option for purely polynomial methods like ours.

There are two main weakness of Newton's method and the Padé iterations: slow convergence in the initial phase and the need to compute explicit inverses. To accelerate initial convergence, Higham popularized the technique of rescaling the matrix after every Newton iteration [21]. Intuitively, rescaling X_t so that $\sigma_{\text{max}} = 1/\sigma_{\text{min}}$ centers the spectrum around 1, where convergence is fastest. Several easily-computable choices of scaling factor exist to accomplish this approximately. Note that this rescaling scheme would fail for Newton-Schulz, which likewise suffers from slow initial convergence but which would diverge if $\sigma_{\text{max}} \gg 1$.

Computing matrix inverses is difficult to parallelize and to implement stably in low precision arithmetic. However, a trick was developed for stably computing many rational methods without explicit inverses; QR decompositions can be used instead [37, 53]. Applying this trick to Halley's method and combining with a special rescaling scheme yields the QDWH (QR-based dynamically weighted Halley) method, which converges in just six iterations for any reasonably conditioned matrix [37].

Adaptive rational methods from optimal approximations. A landmark 2016 paper introduced a new paradigm to design iterative methods for computing polar(M) [38]. We describe this paradigm in more detail in Section 4, but the main insight is as follows. Padé methods choose the update rule to be an approximation to $\operatorname{sign}(x)$ of a given degree that is optimally accurate in the neighborhood of x=1. Instead, we should choose the approximation to $\operatorname{sign}(x)$ that is optimal over an $\operatorname{interval}[\ell,1] \subset \mathbb{R}_{\geq 0}$ that contains the singular values. Moreover, after each step of the algorithm, the range of the singular values changes; therefore, we adapt the update rule at each iteration to match the new interval. When the range of the singular values is large, this approach ensures that the update rule shrinks it as quickly as possible. As the algorithm proceeds and the interval shrinks to a small neighborhood of 1, the update rule approaches that of a Padé method, maintaining the same high order of convergence as it has.

Within the class of odd rational functions whose numerators and denominators have degree 2q + 1 and 2q, respectively, an explicit formula for this optimal approximation to $\operatorname{sign}(x)$ on any interval $[\ell, 1]$ was found by Zolotarev. It was shown that these rationals have remarkable convergence properties for any q [38]. For q = 1, this optimal approximation coincides exactly with the dynamically weighted Halley's method (QDWH) referenced above. For even faster convergence than QDWH, [38] proposed the Zolo-pd method, which uses q = 17. Finally, these methods all admit the same QR-based implementation trick as QDWH.

Adaptive polynomial methods. In this paper, we adopt the paradigm of Zolo-pd [38] but with polynomials rather than rationals of degree (2q + 1, 2q). This choice avoids the need for QR factorizations, relying solely on GPU-friendly matrix-matrix multiplications in low-precision arithmetic. While this class of methods has not been fully developed in the numerical analysis literature, similar ideas have been rediscovered in different guises. In an unpublished manuscript that predates Zolo-pd, Chen and Chow [12] describe a rescaling strategy for Newton-Schulz. Though motivated differently, their method is equivalent to ours for degree-3 polynomials (unlike our work, they do not consider general odd degree). They also observe numerical instability that prevents the method from converging to all the way to machine precision. Using the insights of [39], they propose a simple mitigation for this issue that we adopt in Section 4.4. Our work gives the approach from [39] a stronger

theoretical foundation that connects to the paradigm of Zolo-pd. Concretely, we prove that choosing an optimal polynomial at each iteration leads to a composed polynomial that is globally optimal in the sense of (6).

Independently, a group of cryptographers developed a similar method for approximating the scalar function sign(x) in the context of homomorphic encryption schemes [32]. Their focus is mainly on tuning the analogues in their setting of the polynomial degree and number of iterations, whereas we focus on demonstrating optimality and efficiently constructing the update polynomials for degree 3 and 5. In addition, we consider matrix-valued inputs in low-precision arithmetic—not scalars in exact arithmetic—and we demonstrate our method's effectiveness within the Muon algorithm for training deep neural networks.

Application within Muon. The designers of Muon realized that, due to the extreme efficiency requirements and lax accuracy requirements of their setting, rational-based methods from the numerical analysis literature are inapplicable. However, polynomial-based iteration schemes can take full advantage of GPUs because they use only matrix-matrix products in half-precision arithmetic, not inverses or QR decompositions. The preference for speed over accuracy motivates methods that aim to quickly produce coarse approximations, even at the cost of asymptotic convergence. Examples include the proposals of Jordan [25] and You [36, 10], as discussed in Section 1.2. Like Chen and Chow [12], Jordan found that convergence in the initial phase can be accelerated by choosing update rules that have a large derivative near zero, so as to increase the small singular values as much as possible at each iteration. You furthermore chose to use different update rules at each iteration, allowing extra flexibility to tune the trade-off between speed and accuracy. Both used degree-5 polynomials that were found through gradient descent on heuristic objective functions. These proposals were previously compared to Newton-Schultz⁵, but never to Chen and Chow's method from [39]. We find that our method (which generalizes [39]) outperforms them all.

Finally, we remark that concurrent work of Grishina, Smirnov, and Rakhuba also proposes an adaptive polynomial method that generalizes [39] and applies it to accelerating Muon [19]. Like [39], this work does not establish global optimality of the composed polynomial as we do in Section 4 or address finite precision considerations.

3 Approximations by Compositions of Polynomials

To design a GPU-friendly method for computing polar(M), we limit ourselves to the following GPU-friendly operations:

- i) Linear combinations: given scalars $\beta, \gamma \in \mathbb{R}$ and matrices \boldsymbol{B} and \boldsymbol{C} , compute $\beta \boldsymbol{B} + \gamma \boldsymbol{C}$,
- ii) Matrix-matrix products: compute BC.

While both these computational primitives are well-suited for parallel computing environments, matrix-matrix products come at a higher computational cost than linear combinations. Therefore, our method attempts to minimize the number of matrix-matrix

⁵Jordan [25] actually compares to $2x - \frac{3}{2}x^3 + \frac{1}{2}x^5$, whereas the true degree-5 Newton-Schulz polynomial is $(15x - 10x^3 + 3x^5)/8$. However, the difference in performance is negligible for the first few iterations.

products. A key observation is that we can compute odd monomials of $M = U\Sigma V^{\mathsf{T}}$ using the following formula:

$$\boldsymbol{M}^{2q+1} := \boldsymbol{U} \boldsymbol{\Sigma}^{2q+1} \boldsymbol{V}^\mathsf{T} = \boldsymbol{M} (\boldsymbol{M}^\mathsf{T} \boldsymbol{M})^q.$$

Hence, for an odd polynomial $p(x) = a_0x + a_1x^3 + \cdots + a_qx^{2q+1}$ we can compute

$$p(\mathbf{M}) := a_0 \mathbf{M} + a_1 \mathbf{M} (\mathbf{M}^\mathsf{T} \mathbf{M}) + \dots + a_q \mathbf{M} (\mathbf{M}^\mathsf{T} \mathbf{M})^q.$$

It has been shown that for an arbitrary polynomial p, one requires $\Theta(\deg(p)^{1/2})$ products to compute $p(\mathbf{M})$ [44]; see also [23] for related work. This compares favorably to the naive approach that forms all monomials in p and then sums them together, which requires $\Omega(\deg(p))$ products. However, if p can be expressed as a composition of T polynomials, each of degree d

$$p = p_T \circ p_{T-1} \circ \dots \circ p_1, \tag{4}$$

then the degree of p is d^T , and $p(\mathbf{M})$ can be efficiently computed recursively by

$$X_0 = M, \quad X_t = p_t(X_{t-1}) \text{ for } t = 1, 2, \dots, T.$$
 (5)

The final iterate is $X_T = p(M)$, which we compute with just O(Td) matrix-matrix products.

Iterative methods for polar(M) can be seen in this light. For instance, the degree-5 Newton-Schulz method uses the polynomial update $p_t(x) = \frac{15}{8}x - \frac{10}{8}x^3 + \frac{3}{8}x^5$ for each t = 1, ..., T. The composition $p = p_T \circ \cdots \circ p_1$ approximates $\operatorname{sign}(x)$, and the approximation error goes to 0 as T grows. In this paper, we ask the following question: what choice of $p_T \circ \cdots \circ p_1$ gives the *best* approximation to $\operatorname{sign}(x)$?

The method we will present is optimal in the following sense: given lower and upper bounds ℓ and u on the singular values of \mathbf{M} , an odd degree $d \in \mathbb{N}$, and the number of iterations $T \in \mathbb{N}$, our method computes the composition $p^*(\mathbf{M})$ that minimizes the worst-case error in the spectral norm. That is,

$$p^{\star} = \underset{\substack{p = p_T \circ p_{T-1} \circ \dots \circ p_1 \\ p_t \in \mathbb{P}_d^{\text{odd}}}}{\operatorname{argmin}} \max_{\substack{\boldsymbol{M} \in \mathbb{R}^{m \times n} \\ \sigma(\boldsymbol{M}) \subset [\ell, u]}} \|\operatorname{polar}(\boldsymbol{M}) - p(\boldsymbol{M})\|_2.$$
 (6)

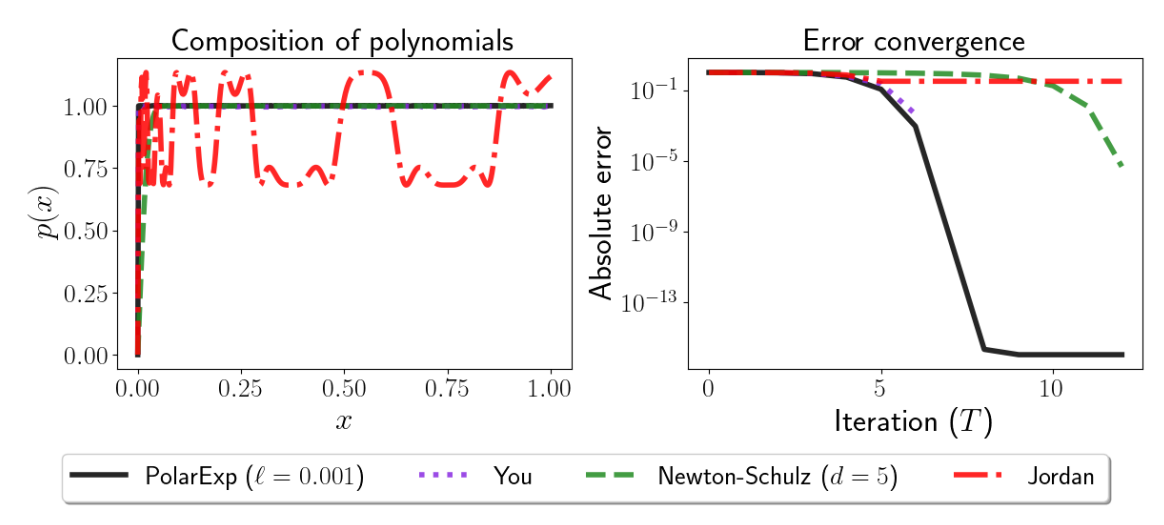
Given that polar $(M) - p(M) = U(I - p(\Sigma))V^{\mathsf{T}}$, and by the unitary invariance of the spectral norm, we have that (6) is equivalent to

$$p^{\star} = \underset{p_{t} \in \mathbb{P}_{d}^{\text{odd}}}{\operatorname{argmin}} \underset{x \in [\ell, u]}{\operatorname{max}} |1 - p(x)|.$$

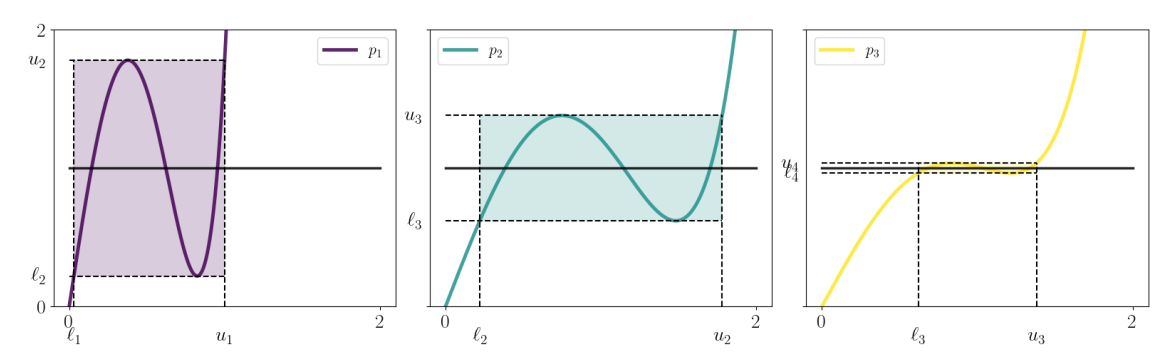
$$(7)$$

For completeness, the equivalence between (6) and (7) is proven in Appendix C.

In other words, the problem given in (6) reduces to that of finding a "uniform" or "minimax" approximation to the constant function $x \mapsto 1$ over the interval $[\ell, u]$, as given in (7). Uniform approximation on an interval by polynomials or rational functions of a given degree is a central topic in approximation theory; see e.g. [50]. Here, we seek an approximation of a particular form—a composition of odd polynomials of fixed degrees. In the next section, we solve the optimization problem of (7) and use the solution to create Polar Express. Figure 2 (a) shows the resulting p^* polynomial labeled as PolarExp, as compared to the Jordan's method in [25], and the six iterations of You's method in [10].



(a) The left figure compares the composition (for T=6 and d=5) of polynomials given by Polar Express ($\ell=0.001$), You's method (which is defined up to 6 iterations), Newton-Schulz, and Jordan's method for approximating $\operatorname{sign}(x)$. The right figure demonstrates the convergence of the methods on [0.001, 1]. Note the slow initial convergence of Newton-Schulz.



(b) The evolution of the first three optimal polynomials p_1 , p_2 , and p_3 and the corresponding lower bounds $\ell_{t+1} = p_t(\ell_t)$ and upper bounds $u_{t+1} = 2 - \ell_{t+1}$, as described in Theorem 4.1. The horizontal black line indicates y = 1. The polynomial degree is d = 5 and the number of iterations is T = 3. We set $\ell_1 = 0.03$ and $u_1 = 1$.

Figure 2

4 The Polar Express

4.1 Greedy is optimal

The key observation is that the polynomial used in each iteration can be chosen greedily, given the choice of polynomials from the previous iterations. For the first iteration, we choose p_1 so as to map the interval $[\ell, u]$ as close to 1 as possible. That is, it minimizes $\max_{x \in [\ell, u]} |1 - p_1(x)|$. The image of p_1 will be a new interval $[\ell_2, u_2]$, where

$$\ell_2 = \min_{x \in [\ell, u]} p_1(x) \qquad u_2 = \max_{x \in [\ell, u]} p_1(x)$$
 (8)

We now pick p_2 to map the interval $[\ell_2, u_2]$ as close to 1 as possible, obtaining a new interval $[\ell_3, u_3]$ that is the image of $[\ell, u]$ through $p_2 \circ p_1$. We continue this process for as many iterations as desired.

The following theorem guarantees that this process finds the solution to (7), and thereby also (6). The scheme is also outlined in Figure 2 (b), which demonstrates the evolution of the lower bounds ℓ_t , the upper bounds u_t , and the polynomials p_t across iterations.

Theorem 4.1. Let d be odd and define $\ell_1 = \ell$ and $u_1 = u$. For $t = 1, \dots, T$ define

$$p_{t} = \underset{p \in \mathbb{P}_{d}^{\text{odd}}}{\operatorname{argmin}} \max_{x \in [\ell_{t}, u_{t}]} |1 - p(x)|$$

$$\ell_{t+1} = \underset{x \in [\ell_{t}, u_{t}]}{\min} p_{t}(x)$$

$$u_{t+1} = \underset{x \in [\ell_{t}, u_{t}]}{\max} p_{t}(x)$$

$$(9)$$

The resulting composition $p^* := p_T \circ p_{T-1} \circ \cdots \circ p_1$ is optimal and the error is given by:

$$\max_{x \in [\ell, u]} |1 - p^{\star}(x)| = \min_{\substack{p = p_T \circ p_{T-1} \circ \dots \circ p_1 \\ p_t \in \mathbb{P}_{\sigma}^{\text{old}}}} \max_{x \in [\ell, u]} |1 - p(x)| = 1 - \ell_{T+1}.$$
 (10)

Furthermore the new error, lower and upper bounds can be computed through

$$\ell_{t+1} = p_t(\ell_t), \quad u_{t+1} = 2 - \ell_{t+1}, \quad \text{and} \quad \max_{x \in [\ell_t, u_t]} |1 - p_t(x)| = 1 - \ell_{t+1}.$$
 (11)

Proof. See Appendix A.

Remark 4.2 (Why a fixed degree?). We note that choice of the degree of each p_1, p_2, \ldots, p_T need not be the same for Theorem 4.1 to hold. More generally, one may specify a sequence of degrees d_1, \ldots, d_T and define each p_t as

$$p_t = \underset{p \in \mathbb{P}_{d_t}^{\text{odd}}}{\operatorname{argmin}} \max_{x \in [\ell_t, u_t]} |p(x) - 1|, \quad \text{for } t = 1, \dots, T.$$

Our theory translates entirely to this more general case. However, for simplicity we assume $d = d_t$ for all t = 1, ..., T. Our setting is similar to that of [32], which considers the closely related problem of choosing the depth T and degrees $d_1, ..., d_T$ such that p approximates sign up to a prescribed error tolerance while minimizing the number of scalar multiplications. Interestingly, from [32, Table 2] the optimal choice of degrees is $d_t = 5$ for almost all iterations. This justifies choosing d to be a constant and our use of d = 5 in particular.

Fortunately, (11) shows that once p_t has been found, we can compute the new lower and upper bounds ℓ_{t+1} and u_{t+1} and the approximation error simply by evaluating $p_t(\ell_t)$. Hence, for any fixed upper and lower bounds on the singular values of M, we can precompute the polynomials p_1, \ldots, p_T and the bounds $[\ell_1, u_1], \ldots, [\ell_{T+1}, u_{T+1}]$. Then, applying the iterative procedure of (5), the final iterate X_T will satisfy the following error bound

$$\|\operatorname{polar}(M) - X_T\|_2 = \|\operatorname{polar}(M) - p^*(M)\|_2 \le 1 - \ell_{T+1}.$$
 (12)

From the optimality guarantee of Theorem 4.1, we know that our method converges at least as fast as the Newton-Schulz iteration of the same degree. Combining this fact

with an existing analysis of Newton-Schulz, we immediately get the following convergence guarantee showing that our method enjoys faster than exponential convergence.

Theorem 4.3. Let M be a matrix normalized so that $\sigma(M) \subset [\ell, 1]$. Let $X_T = p^*(M)$, where p^* is the polynomial from Theorem 4.1 with d = 2q + 1. Then, we have

$$\|\operatorname{polar}(\boldsymbol{M}) - \boldsymbol{X}_T\|_2 \le |1 - \ell^2|^{(q+1)^T}.$$
 (13)

Hence, for d=3 the method converges quadratically and for d=5 the method converges cubically.

Proof. See Appendix B.

In fact, Theorem 4.3 underestimates how fast our method converges. For degree d=5, our method converges about twice as fast as Newton-Schulz (compare with [12, Section 3.1]). Furthermore, the same analysis applies even if p^* is constructed using a "lower bound" ℓ that was too high. That is, replacing ℓ on the right-hand side of (13) by σ_{\min} , the theorem holds even if p^* is constructed to be optimal on the interval $[\ell,1]$ for $\ell > \sigma_{\min}$. Intuitively, when $\ell = u = 1$, the polynomial p^* coincides exactly with the Newton-Schulz method. Mistakenly setting $\ell > \sigma_{\min}$, we obtain a polynomial that converges slower than the optimal polynomial but faster than Newton-Schulz, so the guarantee of Theorem 4.3 still holds (cf. [12, Theorem 3.3]).

4.2 Finding the optimal polynomial for each iteration

Theorem 4.1 shows that we can solve (7) by greedily choosing the optimal approximation $p_t \in \mathbb{P}_d^{\text{odd}}$ for each interval $[\ell_t, u_t]$ for $t = 1, \ldots, T$. In this section, we show how to find each p_t . Since we are now focused on just one iteration, we drop the subscripts. Given ℓ and u, we wish to solve the following optimization problem:

$$\underset{p \in \mathbb{P}_d^{\text{odd}}}{\operatorname{argmin}} \max_{x \in [\ell, u]} |1 - p(x)| \tag{14}$$

That is, we seek a minimax or uniform approximation of the function $x \mapsto 1$ on $[\ell, u]$ from the set of odd polynomials. (Equivalently, we seek a minimax optimal approximation to $\operatorname{sign}(x)$ on $[-u, -\ell] \cup [\ell, u]$.)

Problems of the form (14) are well-studied in approximation theory and numerical analysis. The key mathematical insight underlying the solution is the Equioscillation Theorem, which we state formally for our setting in Lemma A.1. This theorem gives a surprising characterization of the optimal solution of (14): an odd p is optimal for degree 2q + 1 if and only if there is a set of q + 2 equioscillating points. This is a set of points at which p achieves its maximum approximation error $\pm E$, and for which the sign of the error alternates. Even if the optimal approximation error E is not known in advance, finding a set of q + 2 equioscillating points for a given E serves as a certificate that no better approximation error is achievable. The Equioscillation Theorem is the basis of the Remez algorithm [42, 43], a general tool that can be used to find (nearly) optimal polynomial approximations of a given degree to any function on any interval. With very minor modifications to handle the constraint that p be odd, Remez can be used to directly solve (14).

However, the Remez algorithm is opaque, complex, and difficult to implement correctly. Fortunately, we do not need the Remez algorithm in its full generality to solve our problem. We seek only low degree polynomials, and the function we wish to approximate is the constant function $f(x) \equiv 1$. For d = 3, we can derive an explicit, closed form solution to (14) using the Equioscillation Theorem. Up to rescaling, the optimal polynomial turns out to be the same one derived in Chen and Chow by different means [12]. For degree d = 5, we present Algorithm 3, a much simpler way of solving (14) that is mathematically equivalent to Remez in our setting. This algorithm is implemented in its entirety in Appendix G.

We briefly describe the solution for d=3. We seek a polynomial of the form $p(x)=ax+bx^3$. The Equioscillation Theorem stipulates that p must have an equioscillating set of size 3. For p to achieve its maximum error at a point x, x must be a local extremum of p(x)-1 on the interval $[\ell,u]$. Thus, for x to be eligible for membership in the equioscillating set, it must either be a true local extremum of p(x)-1 that happens to lie in $[\ell,u]$, or else one of the endpoints ℓ,u . However, because p is an odd cubic, it has at most one true local extremum on $\mathbb{R}_{\geq 0}$. Thus, to build an equioscillating set of three points, we must include p's unique positive local extremum and both endpoints. This local extremum of p occurs at $\sqrt{\frac{-a}{3b}}$. Therefore, we seek a,b such that

$$p(\ell) = 1 - E,$$
 $p\left(\sqrt{\frac{-a}{3b}}\right) = 1 + E,$ $p(u) = 1 - E$ (15)

for some E. This is a system of three equations in three variables. The solution $p(x) = ax + bx^3$ is most easily expressed as follows. Let $p_{NS}(x) = \frac{3}{2}x - \frac{1}{2}x^3$. Then

$$p(x) = \beta p_{\text{NS}}(\alpha x)$$
, where $\alpha = \sqrt{\frac{3}{u^2 + lu + \ell^2}}$ and $\beta = \frac{4}{2 + \ell u(\ell + u)\alpha^3}$.

We now turn to the degree-5 case. The intuition of Algorithm 3 is as follows. For any fixed set of four points $\ell < q < r < u$, we can find a degree-5 odd polynomial $p(x) = ax + bx^3 + cx^5$ that satisfies

$$p(\ell) = 1 - E,$$
 $p(q) = 1 + E,$ $p(r) = 1 - E,$ $p(u) = 1 + E$

for some E by solving a 4×4 linear system in a, b, c and E. Likewise, for any fixed degree-5 odd p, we can find its four (or fewer) local extrema on $[\ell, u]$ as follows: they occur at ℓ, u and the roots of p', which is an even degree-4 polynomial whose roots can easily be found by the quadratic formula. Algorithm 3 simply alternates between these two steps (solving for a, b, c, E and solving for q, r) until the points q, r converge. Once they have converged, $\{\ell, q, r, u\}$ forms an equioscillating set, so p is the optimal polynomial. For more details, please see Appendix D.

4.3 Upper and lower bounds on the singular values

To instantiate our method, we need upper and lower bounds u and ℓ on the singular values of the input matrix M. A trivial upper bound is given by $||M||_{F}$. For $M \in \mathbb{R}^{m \times n}$ with $n \leq m$, this can overestimate $\sigma_{\max}(M)$ by a factor of \sqrt{n} in the worst case. However in practice, the gradient matrices of the weights of dense linear layers in neural networks tend to have small effective rank [52]. Consequently, the Frobenius norm tends to be a

reasonably good bound on the spectral norm that is loose only by a small constant factor. We rescale the input matrix by setting $X_0 = M/\|M\|_F$ so that u = 1.

It is difficult to efficiently find a good lower bound on the smallest singular value, so we are forced to guess. Fortunately, the consequences of a bad guess are not severe. As discussed above, the method will eventually converge for any $\ell \in (0, u]$, and even an order of magnitude error in our guess of ℓ only delays convergence by a few iterations. For matrices stored in floating point arithmetic, the singular values are usually larger than machine precision ϵ_{mach} [7], so a good guess is to set $\ell \approx \epsilon_{\text{mach}}$. In our numerical experiments we work in bfloat16 where $\epsilon_{\text{mach}} = 2^{-7} = 0.0078125$. Hence we set $\ell = 10^{-3}$ and u = 1. Since we use these bounds for all input matrices, we can precompute the optimal polynomials once and apply them to as many inputs as we want.

4.4 Finite precision considerations

When working in finite-precision arithmetic, especially the half-precision bfloat16 format used in deep learning, we must take some care to avoid blowups and other problems due to numerical error. To this end, we make three small changes to the method. These adjustments stabilize the algorithm with a negligible effect on accuracy. Furthermore, these adjustments can be made in the offline stage by modifying the coefficients of our optimal polynomials.

The first issue arises when numerical round-off creates singular values that are slightly larger than our current upper bound u_t . Our optimal polynomials converge only when the singular values of X_t are less than u_t . In some cases we have

$$p_t(u_t + \epsilon) > u_{t+1} + \epsilon$$
,

so over many iterations, a singular value that is slightly larger than u_t large could grow to ∞ instead of converging to 1.

To fix this issue, we simply replace each polynomial $x \mapsto p_t(x)$ by $x \mapsto p_t(x/1.01)$.

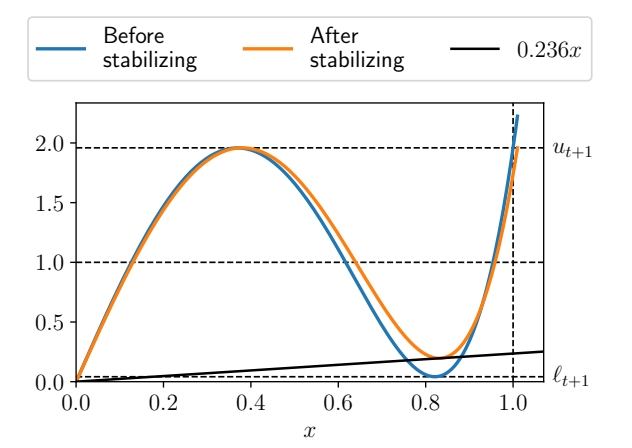


Figure 3: Effects of stabilizing the update rules with a safety factor and cushioning, as described in Section 4.4. The blue curve is the optimal degree-5 polynomial for the interval [0.005, 1]. It is has numerical issues because it maps singular values near 0.8 down to almost zero and maps $1 + \epsilon$ to $\approx u_{t+1} + 25\epsilon$. The stabilized version is better because it ensures $\frac{p_t(x)}{x} \geq 0.236$ and maps all $x \leq 1.01$ to at most u_{t+1} .

This safety factor corrects for round-off errors in previous iterations while only slightly changing the behavior of the polynomial on the interval $[\ell_t, u_t]$, though it does cause the singular values to converge to 0.999998 instead of to 1. To correct for this, the safety factor can be omitted in the final iteration.

The second issue was identified in [39] and addressed in the context of polynomial iterations by Chen and Chow [12]. In general, iterative methods for polar(M) aim to increase each singular value relative to the largest singular value; while $\sigma_{\min}(X_0) \ll \sigma_{\max}(X_0)$, after enough iterations, $\sigma_{\min}(X_t) \approx \sigma_{\max}(X_t) \approx 1$. However, the convergence of each singular value to σ_{\max} may not be monotonic. Over the domain $[\ell_t, u_t]$, our optimal polynomial p_t oscillates repeatedly between ℓ_{t+1} and u_{t+1} , so some singular values that are

near u_t may get mapped down to ℓ_{t+1} . It so happens that this non-monotonicity—even at a single iteration—can cause loss of precision. That is, problems occur if

$$\frac{p_t(\sigma_i)}{\sigma_i} \ll \frac{\max\limits_{x \in [\sigma_{\min}, \sigma_{\max}]} p_t(x)}{\sigma_{\max}},$$

where $0 \le \sigma_{\min} \le \sigma_i \le \sigma_{\max}$ are singular values of X_t [39]. In the extreme case $p_t(\sigma_i) < 0$, the *i*th singular vector will change sign, casuing the method to converge to the polar factor of the wrong matrix. Unlike Newton-Schulz, unscaled Newton, or QDWH, our method is affected by this loss of precision.

To mitigate this issue, [12] propose modifying their update polynomials to enforce a lower bound on the ratio $\frac{p_t(\sigma_i)}{\sigma_i}$. This issue only occurs when $\ell_t \ll u_t$; as $\ell_t \to u_t$, our optimal polynomial approaches the Padé approximant and so $\frac{p_t(x)}{x} \geq 1$ for all $x \in [0, u_t]$. We could fully solve the problem by using the Padé approximant instead of our optimal polynomial, but this would significantly slow down convergence. Instead we compromise. When $\ell_t \geq u_t/10$, we find that $\frac{p_t(x)}{x} \geq 0.236$. Therefore, whenever $\ell_t < u_t/10$ we select the update rule as though $\ell_t = u_t/10$. This change slows convergence, but only very slightly. (The choice of 10 is somewhat arbitrary. In Appendix G, we use a different factor.)

The third change is copied from the original Muon implementation: normalize M by $\|M\|_{\rm F} + 10^{-2}$ instead of by $\|M\|_{\rm F}$. As before, we set $u_1 = 1$.

4.5 The algorithm

12

13 end for

14 return X_T .

 $X_t = p_t(X_{t-1})$

```
Algorithm 2 The General Polar Express input: Matrix M, iteration count T, degree d, approximate lower bound \ell. output: An approximation X_T to polar(M).
```

We give the pseudocode of our proposed method for any degree in Algorithm 2 and provide a complete implementation in our repository. We give the specific version of the Polar Express with degree d=5 and $\ell=$ 10^{-3} used in our GPT experiments in Algorithm 1. Our algorithm first computes the polynomials p_1, \ldots, p_T of Theorem 4.1 in full precision using the results of Section 4.2 (or the Remez algorithm for d > 5). This stage is offline because the coefficients of the polynomials are only computed and stored once. For every subsequent call to the algorithm, these coefficients are reused and the offline stage is skipped. For instance, in Algorithm 1 these polynomials have been precomputed and stored in the variable coeffs_list.

The polynomial $p^* := p_T \circ \cdots \circ p_1$ is then applied to the input matrix M in the online stage. The online stage can be performed in lower precision (bfloat16) for greater speed on a GPU. Horner's rule can be used to carry out each iteration. For instance, if

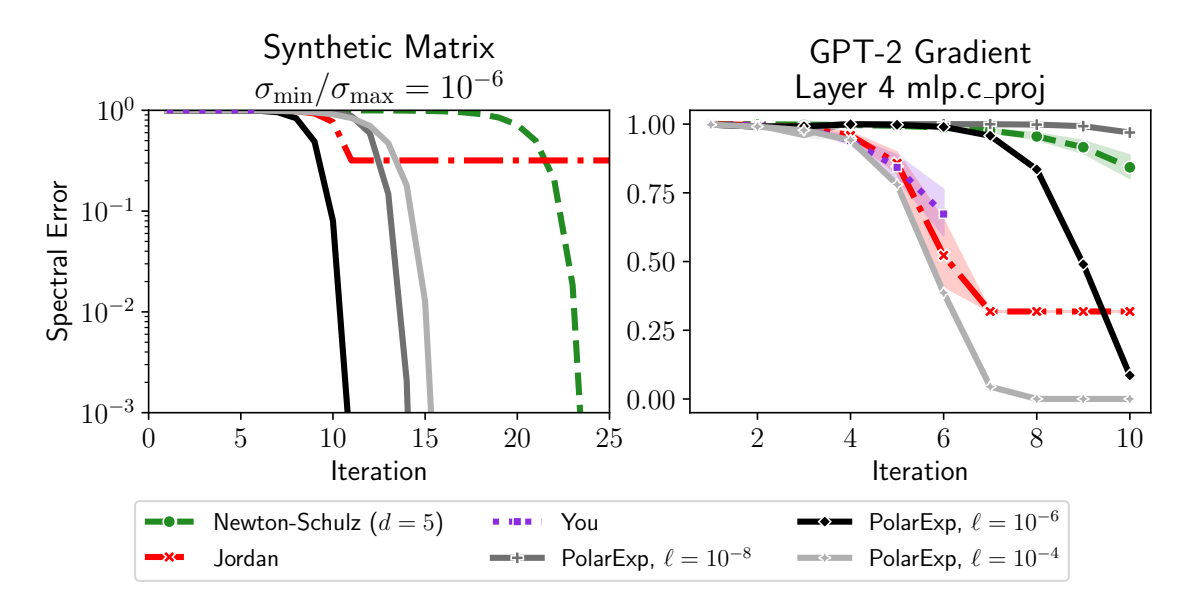


Figure 4: Convergence of various degree-5 polynomial methods in the spectral norm. When tuned properly, Polar Express attains outperforms the other methods at every iteration. Left panel: synthetic matrix with $\sigma_{\text{max}} = 1$, $\sigma_{\text{min}} = 10^{-6}$. Right panel: gradient of a certain weight matrix of a randomly-initialized GPT-2 architecture on a batch of language modeling data, normalized by the Frobenius norm.

 $p_t = ax + bx^3 + cx^5$, then

$$\boldsymbol{X}_{t} = \boldsymbol{X}_{t-1} \left(a \boldsymbol{I} + \boldsymbol{Y}_{t-1} \left(b \boldsymbol{I} + c \boldsymbol{Y}_{t-1} \right) \right)$$

where
$$Y_{t-1} = X_{t-1}^{\top} X_{t-1}$$
.

A simple implementation of the offline stage of Algorithm 2 is given in Appendix G. For deep learning applications, we recommend using d=5 and T=5 or 6 with $\ell_1=10^{-3}$. With these parameters, the offline stage as implemented in Appendix G gives the polynomials encoded in coeffs_list in Algorithm 1. All told, our proposal for Muon is to apply the composition of these polynomials to $M/(\|M\|_F + 10^{-2})$.

5 Numerical Experiments

5.1 Convergence of Polar Express

We compare the performance of Polar Express against degree-5 Newton-Schulz and the methods of Chen and Chow [12], Jordan [25], and You [10].

We first study an idealized scenario where the spectrum of the input matrix is known exactly. We generate a random matrix whose singular values are evenly spaced on a logarithmic scale between 10^{-6} and 1. The right and left singular vectors are chosen at random. The left panel of Figure 4 shows the results. Since all the methods in this plot use degree-5 polynomials, their computational and runtime costs are all proportional to the number of iterations. As expected, Newton-Schulz converges but makes almost no progress for the first 17 iterations. Jordan's method rapidly achieves an error of ≈ 0.3 after just 11 iterations, but ceases to converge further. You's method, which is difficult to

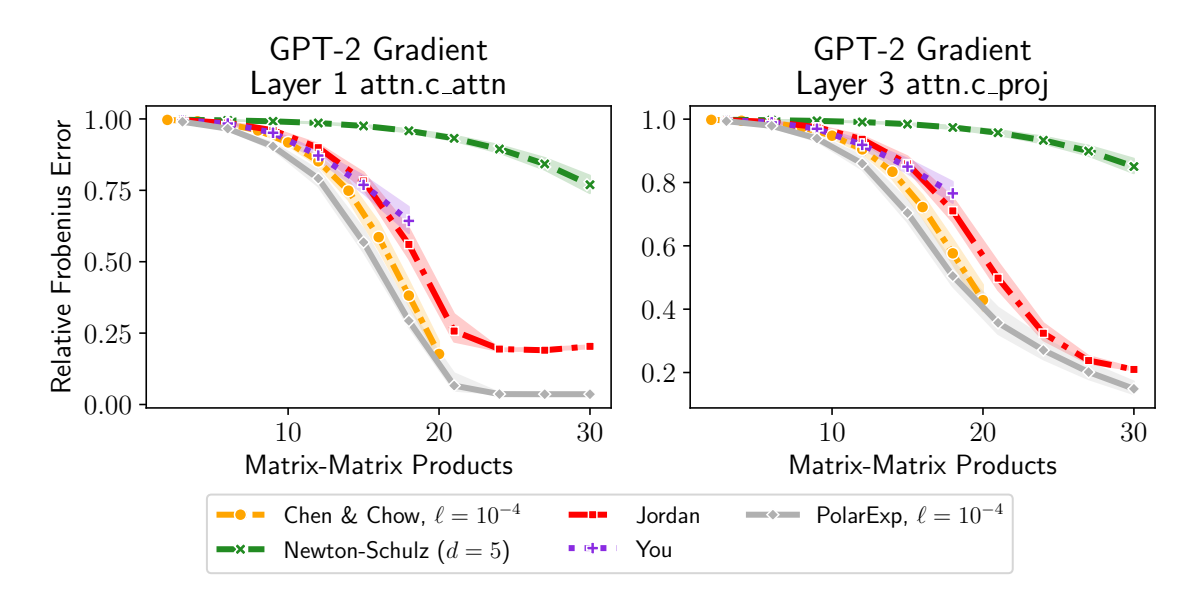


Figure 5: Convergence of polynomial methods in the Frobenius norm on GPT-2 gradient matrices. The number of matrix-matrix products is T(d+1)/2, where d is the degree (3 for Chen & Chow; 5 for all others) and T is the number of iterations.

see on the plot because it is only defined for six iterations, converges at a similar rate as Jordan's method. When Polar Express is instantiated with $\ell = \sigma_{\min}$, it dominates the other methods at every iteration, achieving excellent accuracy after just 11 iterations and converging about twice as fast as Newton-Schulz to any given error. Even when the lower bound on σ_{\min} is wrong by two orders of magnitude in either direction, the method remains competitive, though it does not actually outperform Jordan's method until iteration 13 or 14.

Next we test the methods' performance on a matrix from a real-world application, namely, the gradient of a weight matrix from the fourth transformer block of a GPT-2 architecture with respect to a language modeling objective on a batch of text from the Tiny Shakespeare dataset [27]. The right panel of Figure 4 shows the results. Once again, the best-tuned version of Polar Express outperforms the other methods. This time, we see that setting ℓ to be many orders of magnitude too small can delay convergence significantly, and make Polar Express less competitive as compared to Jordan's method.

For most other weight matrices in this GPT-2 model, the methods all take more than 10 iterations to converge in the spectral norm. The spectral error is large if there is even one outlying singular value that is far from 1. However, for some applications, we may be satisfied with a weaker notion of convergence, like the relative Frobenius norm. Figure 5 shows the performance of various methods on this metric. We use gradient matrices of the same model, but from two different layers. In addition, we compare the degree-5 methods to Chen and Chow's degree-3 method. To make this comparison fair, we measure the number of matrix-matrix products performed by each method instead the number of iterations. We find that Polar Express can once again dominate the other methods across iterations. Chen and Chow's method is also quite competitive, and the remaining methods behave much as in Figure 4.

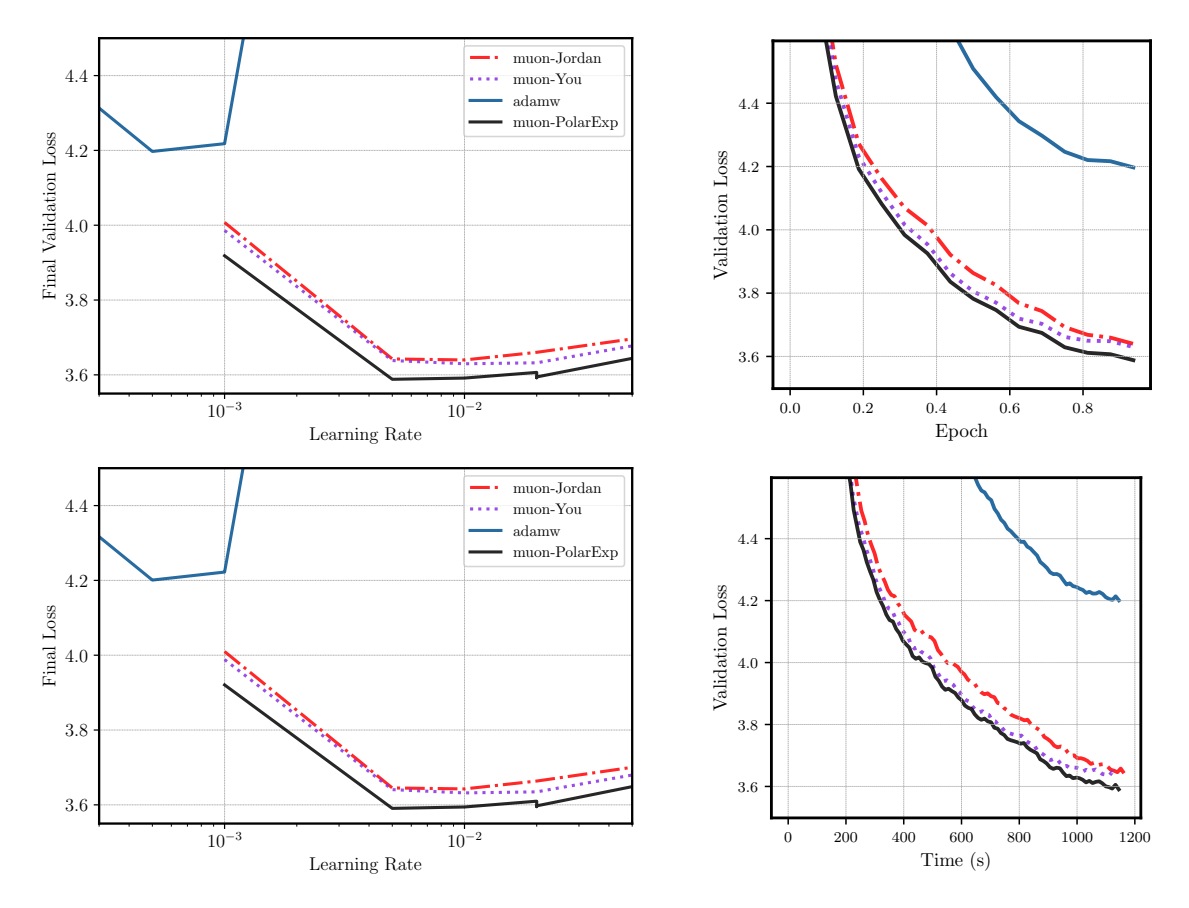


Figure 6: Training a GPT-2 (124M) model on 1 Billion tokens of the Fineweb data set [2]. The Legend muon-<name> refers to using muon with the <name> method for computing polar(M) with weight decay zero. Top Left: The final validation loss vs. the learning rate. The final best validation losses for each method were, in reverse order, adamw: 4.197, muon-Jordan: 3.639, muon-You: 3.629 and muon-PolarExp: 3.588. Bottom Left: The final training loss vs the learning rate. Top Right: Validation loss vs. number of iterations. Bottom Left: validation loss vs. time, plotting each method with its best learning rate.

5.2 Training GPT-2

In our final experiment, we compare the performance of using our Polar Express method given in Algorithm 1 inside the Muon algorithm versus Jordan's [25] and You's [10] methods.⁶ We train two different GPT-2 models:

$$\begin{split} \text{GPT-Small:} \quad n_{\text{embd}} = 768, \quad n_{\text{layer}} = 12, \quad n_{\text{head}} = 12 \\ \text{GPT-Large:} \quad n_{\text{embd}} = 1280, \quad n_{\text{layer}} = 36, \quad n_{\text{head}} = 20 \end{split}$$

and a vocabulary size of 50,257, using a context length of 1024. Training is performed on 1B tokens from the FineWeb dataset [2], using a batch size of 32 and a single epoch. All models are trained with mixed precision (bfloat16) on 4 H100 GPUs. For all methods we use the learning rate schedule proposed in [24], consisting of a constant phase for the first 40% of training steps followed by a linear decay. All methods for the matrix sign computations are performed in float16b precision and use five iterations.

⁶Our code is available at https://github.com/modichirag/GPT-opt/tree/polar, in the polar branch.

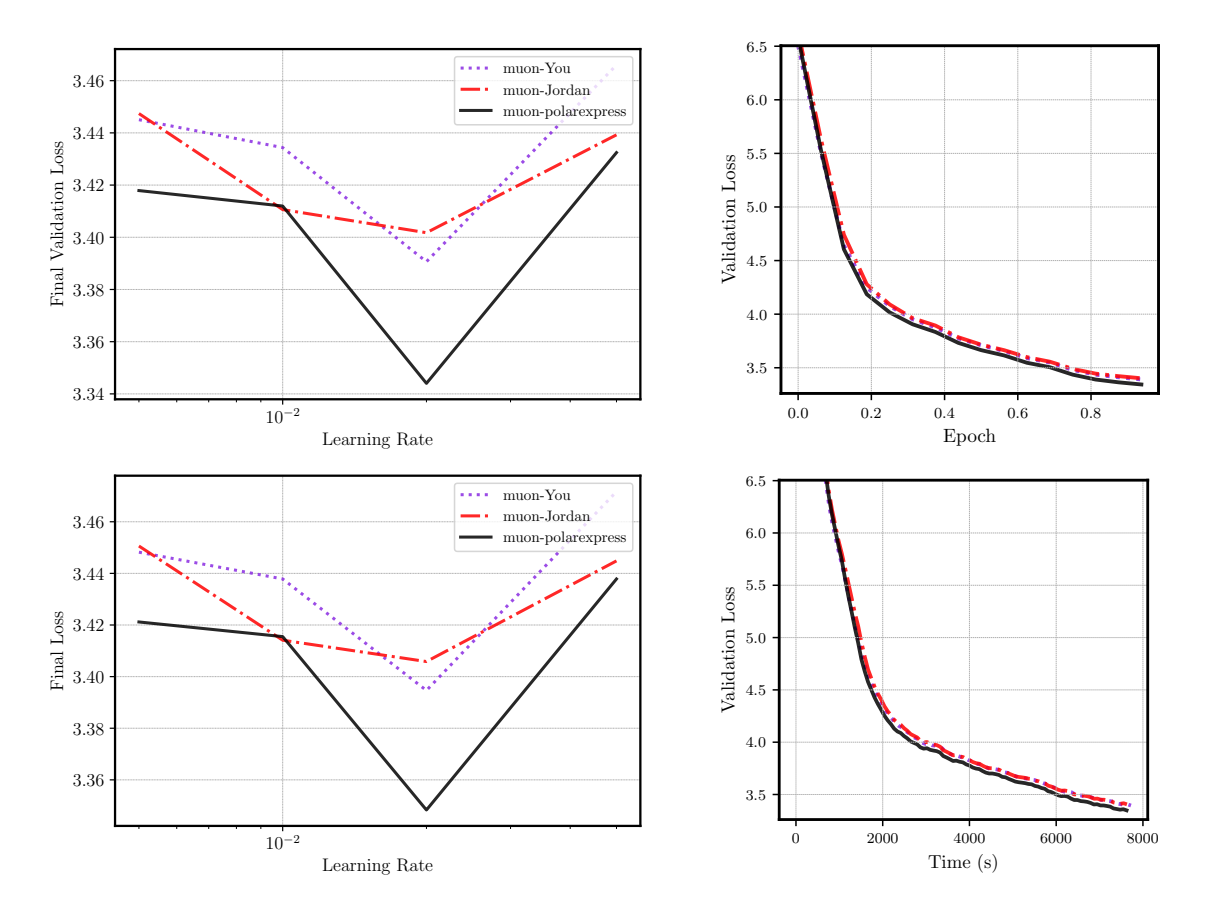


Figure 7: Training a GPT-2-Large model (774M params) on 1 Billion tokens of the Fineweb data set [2]. The Legend muon-<name> refers to using muon with the <name> method for computing polar(M). We used weight decay 0.1 for all methods. Top Left: The final validation loss vs. the learning rate. The final best validation losses for each method were, in reverse order, adamw: 4.197, muon-Jordan: 3.639, muon-You: 3.629 and muon-PolarExp: 3.588. Bottom Left: The final training loss vs the learning rate. Top Right: Validation loss vs. number of iterations. Bottom Left: validation loss vs. time, plotting each method with its best learning rate.

We apply Muon selectively to certain layers of the model. Following the nano-gpt implementation [24], we assign Muon to all parameters with at least two dimensions (typically weight matrices, and excluding RMS norm parameters), excluding the embeddings, unembeddings, and the positional encodings. These excluded parameters are instead optimized with AdamW.

Figure 1 and Figure 6 shows the resulting runs of each method in terms of validation loss and training loss on the GPT-Large and GPT-Small models, respectively. In both figures we can see that muon-PolarExp achieves a better validation and training loss than muon-Jordan or muon-You for every learning rate. Since each iteration of the different matrix sign methods are equally expensive (since they all apply a degree 5 polynomial), improved validation loss in terms of epochs also translates to an improved loss in terms of wall clock time (see bottom right of Figure 6). The advantage is remarkably consistent across all learning rates and epochs.

We also experimented with adding weight decay 0.1 to the model, keeping all else the

same, in Figure 7. Here we find again that muon-PolarExp achieves a better validation and training loss for every learning rate, except one $(lr = 10^{-2})$ where its performance matches that of muon-Jordan.

Acknowledgements

This work was partially supported by NSF awards 2045590 and 2234660. Computations were run at facilities supported by the Scientific Computing Core at the Flatiron Institute, a division of the Simons Foundation.

References

- [1] N. I. Achieser. *Theory of approximation*. Dover Publications, Inc., New York, 1992. Translated from the Russian and with a preface by Charles J. Hyman, Reprint of the 1956 English translation.
- [2] Samuel Aroca-Ouellette, Philippe Beaudoin, Guillaume Lajoie, Liam Paull, Joelle Pineau, Pascal Vincent, and Anirudh Goyal. Fineweb: Learning language models with high quality web data. In *NeurIPS Datasets and Benchmarks Track*, 2023. URL: https://arxiv.org/abs/2306.03061.
- [3] Michele Benzi and Ru Huang. Some matrix properties preserved by generalized matrix functions. Spec. Matrices, 7:27–37, 2019. doi:10.1515/spma-2019-0003.
- [4] Jeremy Bernstein and Laker Newhouse. Modular duality in deep learning. arXiv preprint arXiv:2410.21265, 2024. URL: https://arxiv.org/abs/2410.21265.
- [5] Jeremy Bernstein and Laker Newhouse. Old optimizer, new norm: An anthology. arXiv preprint arXiv:2409.20325, 2024. URL: https://arxiv.org/abs/2409.20325.
- [6] Å. Björck and C. Bowie. An iterative algorithm for computing the best estimate of an orthogonal matrix. SIAM J. Numer. Anal., 8:358–364, 1971. doi:10.1137/0708036.
- [7] Christos Boutsikas, Petros Drineas, and Ilse C. F. Ipsen. Small singular values can increase in lower precision. SIAM J. Matrix Anal. Appl., 45(3):1518–1540, 2024. doi:10.1137/23M1557209.
- [8] David Carlson, Volkan Cevher, and Lawrence Carin. Stochastic Spectral Descent for Restricted Boltzmann Machines. In Guy Lebanon and S. V. N. Vishwanathan, editors, Proceedings of the Eighteenth International Conference on Artificial Intelligence and Statistics, volume 38 of Proceedings of Machine Learning Research, pages 111–119, San Diego, California, USA, 09–12 May 2015. PMLR. URL: https://proceedings.mlr.press/v38/carlson15.html.
- [9] David E Carlson, Edo Collins, Ya-Ping Hsieh, Lawrence Carin, and Volkan Cevher. Preconditioned spectral descent for deep learning. In C. Cortes, N. Lawrence, D. Lee, M. Sugiyama, and R. Garnett, editors, Advances in Neural Information Processing Systems, volume 28. Curran Associates, Inc., 2015. URL: https://proceedings.neurips.cc/paper_files/paper/2015/file/f50a6c02a3fc5a3a5d4d9391f05f3efc-Paper.pdf.

- [10] Franz Louis Cesista, You Jiacheng, and Keller Jordan. Squeezing 1-2% efficiency gains out of muon by optimizing the newton-schulz coefficients, 2025. URL: http://leloykun.github.io/ponder/muon-opt-coeffs/.
- [11] PL Chebyshev. Questions on smallest quantities connected with the approximate representation of functions (1859). *Collected works*, 2:151–235, 1947.
- [12] Jie Chen and Edmond Chow. A stable scaling of newton-schulz for improving the sign function computation of a hermitian matrix. *Preprint ANL/MCS-P5059-0114*, 2014. URL: https://www.mcs.anl.gov/papers/P5059-0114.pdf.
- [13] E. W. Cheney. *Introduction to approximation theory*. McGraw-Hill Book Co., New York-Toronto-London, 1966.
- [14] J. Douglas Carroll and Phipps Arabie. Chapter 3 multidimensional scaling. In Michael H. Birnbaum, editor, Measurement, Judgment and Decision Making, Handbook of Perception and Cognition (Second Edition), pages 179–250. Academic Press, San Diego, 1998. URL: https://www.sciencedirect.com/science/article/pii/ B9780120999750500051, doi:10.1016/B978-012099975-0.50005-1.
- [15] John Duchi, Elad Hazan, and Yoram Singer. Adaptive subgradient methods for online learning and stochastic optimization. *J. Mach. Learn. Res.*, 12:2121–2159, 2011.
- [16] Alexandre Eremenko and Peter Yuditskii. Uniform approximation of sgn x by polynomials and entire functions. *J. Anal. Math.*, 101:313–324, 2007. doi:10.1007/s11854-007-0011-3.
- [17] Gene H. Golub and Charles F. Van Loan. Matrix computations. Johns Hopkins Studies in the Mathematical Sciences. Johns Hopkins University Press, Baltimore, MD, fourth edition, 2013.
- [18] J. C. Gower and G. B. Dijksterhuis. Procrustes problems, volume 30 of Oxford Statistical Science Series. Oxford University Press, Oxford, 2004. doi:10.1093/ acprof:0so/9780198510581.001.0001.
- [19] Ekaterina Grishina, Matvey Smirnov, and Maxim Rakhuba. Accelerating newton-schulz iteration for orthogonalization via chebyshev-type polynomials, 2025. URL: https://arxiv.org/abs/2506.10935, arXiv:2506.10935.
- [20] Vineet Gupta, Tomer Koren, and Yoram Singer. Shampoo: Preconditioned stochastic tensor optimization. In Jennifer Dy and Andreas Krause, editors, *Proceedings of the 35th International Conference on Machine Learning*, volume 80 of *Proceedings of Machine Learning Research*, pages 1842–1850. PMLR, 10–15 Jul 2018. URL: https://proceedings.mlr.press/v80/gupta18a.html.
- [21] Nicholas J. Higham. Computing the polar decomposition—with applications. SIAM J. Sci. Statist. Comput., 7(4):1160–1174, 1986. doi:10.1137/0907079.
- [22] Nicholas J. Higham. Functions of matrices. SIAM, Philadelphia, PA, 2008. doi: 10.1137/1.9780898717778.

- [23] Elias Jarlebring and Gustaf Lorentzon. The polynomial set associated with a fixed number of matrix-matrix multiplications. arXiv preprint arXiv:2504.01500, 2025. URL: https://arxiv.org/abs/2504.01500.
- [24] Keller Jordan, Jeremy Bernstein, Brendan Rappazzo, @fernbear.bsky.social, Boza Vlado, You Jiacheng, Franz Cesista, Braden Koszarsky, and @Grad62304977. modded-nanogpt: Speedrunning the nanogpt baseline, 2024. URL: https://github.com/KellerJordan/modded-nanogpt.
- [25] Keller Jordan, Yuchen Jin, Vlado Boza, Jiacheng You, Franz Cesista, Laker Newhouse, and Jeremy Bernstein. Muon: An optimizer for hidden layers in neural networks, 2024. URL: https://kellerjordan.github.io/posts/muon/.
- [26] Tetsuya Kaneko, Simone Fiori, and Toshihisa Tanaka. Empirical arithmetic averaging over the compact Stiefel manifold. *IEEE Trans. Signal Process.*, 61(4):883–894, 2013. doi:10.1109/TSP.2012.2226167.
- [27] Andrej Karpathy. char-rnn. https://github.com/karpathy/char-rnn, 2015.
- [28] Charles Kenney and Alan J. Laub. Rational iterative methods for the matrix sign function. SIAM J. Matrix Anal. Appl., 12(2):273–291, 1991. doi:10.1137/0612020.
- [29] Kimi Team, Yifan Bai, Yiping Bao, Guanduo Chen, Jiahao Chen, Ningxin Chen, Ruijue Chen, Yanru Chen, Yuankun Chen, Yutian Chen, Zhuofu Chen, et al. Kimi k2: Open agentic intelligence, 2025. URL: https://arxiv.org/abs/2507.20534, arXiv:2507.20534.
- [30] Diederik P. Kingma and Jimmy Ba. Adam: A method for stochastic optimization. In *International Conference on Learning Representations*, 2015. URL: http://arxiv.org/abs/1412.6980.
- [31] Zdislav Kovářík. Some iterative methods for improving orthonormality. SIAM J. Numer. Anal., 7:386–389, 1970. doi:10.1137/0707031.
- [32] Eunsang Lee, Joon-Woo Lee, Jong-Seon No, and Young-Sik Kim. Minimax approximation of sign function by composite polynomial for homomorphic comparison. *IEEE Transactions on Dependable and Secure Computing*, 19(6):3711–3727, 2022. doi:10.1109/TDSC.2021.3105111.
- [33] R. B. Leipnik. Rapidly convergent recursive solution of quadratic operator equations. Numer. Math., 17:1–16, 1971. doi:10.1007/BF01395861.
- [34] Jingyuan Liu, Jianlin Su, Xingcheng Yao, Zhejun Jiang, Guokun Lai, Yulun Du, Yidao Qin, Weixin Xu, Enzhe Lu, Junjie Yan, et al. Muon is scalable for LLM training. arXiv preprint arXiv:2502.16982, 2025. URL: https://arxiv.org/abs/2502.16982.
- [35] Ilya Loshchilov and Frank Hutter. Decoupled weight decay regularization. In *International Conference on Learning Representations*, 2019. URL: https://openreview.net/forum?id=Bkg6RiCqY7.
- [36] Modula. Newton-schulz algorithm jiacheng's six-step method. https://docs.modula.systems/algorithms/newton-schulz/#jiacheng-s-six-step, 2024. Accessed: 2025-05-19.

- [37] Yuji Nakatsukasa, Zhaojun Bai, and François Gygi. Optimizing Halley's iteration for computing the matrix polar decomposition. SIAM J. Matrix Anal. Appl., 31(5):2700– 2720, 2010. doi:10.1137/090774999.
- [38] Yuji Nakatsukasa and Roland W. Freund. Computing fundamental matrix decompositions accurately via the matrix sign function in two iterations: the power of Zolotarev's functions. SIAM Rev., 58(3):461–493, 2016. doi:10.1137/140990334.
- [39] Yuji Nakatsukasa and Nicholas J. Higham. Backward stability of iterations for computing the polar decomposition. SIAM J. Matrix Anal. Appl., 33(2):460–479, 2012. doi:10.1137/110857544.
- [40] Yuji Nakatsukasa and Nicholas J. Higham. Stable and efficient spectral divide and conquer algorithms for the symmetric eigenvalue decomposition and the SVD. SIAM J. Sci. Comput., 35(3):A1325-A1349, 2013. doi:10.1137/120876605.
- [41] Herbert Neuberger. Exactly massless quarks on the lattice. *Phys. Lett. B*, 417(1-2):141–144, 1998. doi:10.1016/S0370-2693(97)01368-3.
- [42] Ricardo Pachón and Lloyd N. Trefethen. Barycentric-Remez algorithms for best polynomial approximation in the chebfun system. *BIT*, 49(4):721–741, 2009. doi: 10.1007/s10543-009-0240-1.
- [43] T Parks and James McClellan. Chebyshev approximation for nonrecursive digital filters with linear phase. *IEEE Transactions on circuit theory*, 19(2):189–194, 1972. doi:10.1109/TCT.1972.1083419.
- [44] Michael S. Paterson and Larry J. Stockmeyer. On the number of nonscalar multiplications necessary to evaluate polynomials. SIAM J. Comput., 2:60–66, 1973. doi:10.1137/0202007.
- [45] Thomas Pethick, Wanyun Xie, Kimon Antonakopoulos, Zhenyu Zhu, Antonio Silveti-Falls, and Volkan Cevher. Training deep learning models with norm-constrained lmos, 2025. URL: https://arxiv.org/abs/2502.07529, arXiv:2502.07529.
- [46] Artem Riabinin, Egor Shulgin, Kaja Gruntkowska, and Peter Richtárik. Gluon: Making muon & scion great again! (bridging theory and practice of lmo-based optimizers for llms), 2025. URL: https://arxiv.org/abs/2505.13416, arXiv:2505.13416.
- [47] Ishaan Shah, Anthony M Polloreno, Karl Stratos, Philip Monk, Adarsh Chaluvaraju, Andrew Hojel, Andrew Ma, Anil Thomas, Ashish Tanwer, Darsh J Shah, et al. Practical efficiency of muon for pretraining. arXiv preprint arXiv:2505.02222, 2025. URL: https://arxiv.org/abs/2505.02222.
- [48] Hao-Jun Michael Shi, Tsung-Hsien Lee, Shintaro Iwasaki, Jose Gallego-Posada, Zhijing Li, Kaushik Rangadurai, Dheevatsa Mudigere, and Michael Rabbat. A distributed data-parallel PyTorch implementation of the distributed Shampoo optimizer for training neural networks at-scale. arXiv preprint arXiv:2309.06497, 2023. URL: https://arxiv.org/abs/2309.06497.
- [49] Attila Szabo and Neil S Ostlund. Modern quantum chemistry: introduction to advanced electronic structure theory. Courier Corporation, 1996.

- [50] Lloyd N. Trefethen. Approximation theory and approximation practice. Society for Industrial and Applied Mathematics (SIAM), Philadelphia, PA, extended edition, 2020.
- [51] Nikhil Vyas, Depen Morwani, Rosie Zhao, Itai Shapira, David Brandfonbrener, Lucas Janson, and Sham M. Kakade. SOAP: Improving and stabilizing shampoo using adam for language modeling. In *The Thirteenth International Conference on Learning Representations*, 2025. URL: https://openreview.net/forum?id=IDxZhXrpNf.
- [52] Greg Yang, James B. Simon, and Jeremy Bernstein. A spectral condition for feature learning, 2024. URL: https://arxiv.org/abs/2310.17813, arXiv:2310.17813.
- [53] Zhenyue Zhang, Hongyuan Zha, and Wenlong Ying. Fast parallelizable methods for computing invariant subspaces of Hermitian matrices. *J. Comput. Math.*, 25(5):583–594, 2007. URL: http://www.jstor.org/stable/43693395.

A Proof of Theorem 4.1

The aim of this section is to prove Theorem 4.1. We begin with a result that provides a few essential properties for the polynomial solving (7) when T = 1. This result is known as Chebyshev's theorem [11] or the equioscillation theorem [50, Chapter 10].

Lemma A.1. Let d = 2q + 1 and $u, \ell > 0$. Consider the problem

$$\min_{p \in \mathbb{P}_d^{\text{odd}}} \max_{x \in [\ell, u]} |1 - p(x)|. \tag{16}$$

There exists a unique polynomial $p^* \in \mathbb{P}_d^{\text{odd}}$ solving (16). Furthermore, p^* is the unique solution to the above problem if and only if there exist q+2 distinct points $\{x_0,\ldots,x_{q+1}\}\subset [\ell,u]$ such that

$$1 - p^{\star}(x_i) = \eta(-1)^i \max_{x \in [\ell, u]} |1 - p^{\star}(x)|, \quad \text{for } i = 0, \dots, q + 1,$$

for $\eta = 1$ or $\eta = -1$.

Proof. A discussion can be found in [16]. Here we include a formal proof for completeness. By Chebyshev's Theorem [1, 11, 13] it is sufficient to show that $\mathbb{P}_d^{\text{odd}}$ satisfies the Haar condition: any non-zero $p \in \mathbb{P}_d^{\text{odd}} = \text{span}\{x,\ldots,x^3,\ldots,x^{2q+1}\}$ can have at most q roots in $[\ell,u]$.

Since $\deg(p)=d=2q+1$ we know that p can have at most 2q+1 roots in \mathbb{R} . However, since p(0)=0 and p(x)=-p(-x) we know that p has one root at zero, and the remaining roots come in symmetric pairs (x,-x). Because of this, p can have at most q roots in the positive orthant, and thus it can have at most q roots in $[\ell,u]\subset(0,\infty)$. Hence, $\mathbb{P}_d^{\mathrm{odd}}$ satisfies the Haar condition, which yields the desired result.

The proof of Theorem 4.1 will be by induction on T. We begin by establishing the base case, T = 1, which is handled by the following result.

Lemma A.2. Let $u, \ell > 0$ and define

$$p^{\star} := \underset{p \in \mathbb{P}_d^*}{\operatorname{argmin}} \max_{x \in [\ell, u]} |1 - p(x)|.$$

Then

$$p^{\star}(\ell) = \min_{x \in [\ell, u]} p^{\star}(x), \quad \max_{x \in [\ell, u]} p^{\star}(x) = 2 - p^{\star}(\ell), \text{ and } \max_{x \in [\ell, u]} |1 - p^{\star}(x)| = 1 - p^{\star}(\ell).$$

Proof. Throughout the proof we assume d = 2q + 1. We begin with proving

$$p^{\star}(\ell) = \min_{x \in [\ell, u]} p^{\star}(x).$$

Consider the polynomial $e(x) := 1 - p^*(x)$. The proof will contain three steps. We first rule out the trivial case that $p^* \neq 0$, since $p(x) = \frac{2}{\ell + u}x$ would then be a better approximation. Hence, p^* cannot be the zero polynomial.

Step 1: e(x) has exactly q stationary points inside the open interval (ℓ, u) .

Note that e(x) has at most 2q stationary points in \mathbb{R} , since its derivative e'(x) is a polynomial of degree 2q. Furthermore, since p^* is odd, we have that e'(x) = -p'(x) is even of degree 2q, and thus can have at most q stationary points contained in $(0, +\infty)$. Hence, there can be at most q stationary points of e(x) inside the interval $[\ell, u]$.

By Lemma A.1 there are q+2 points $x_0,\ldots,x_{q+1}\in [\ell,u]$ where e(x) is maximized or minimized in $[\ell,u]$. These points are either stationary points or they are endpoints of the interval $[\ell,u]$. Let $n_{\rm ext}$ be the number of stationary points and $n_{\rm stat}$ be the number of endpoints in the set $\{x_0,\ldots,x_{q+1}\}$. Since a point can be both a stationary point and an endpoint we have $q+2\leq n_{\rm end}+n_{\rm stat}$. However, $n_{\rm end}\leq 2$ and $n_{\rm stat}\leq q$, which follows from the previous paragraph where we showed that there are at most q stationary points of e(x) in $[\ell,u]$. So $n_{\rm end}+n_{\rm stat}\leq q+2$, and consequently we must have $n_{\rm end}=2$ and $n_{\rm stat}=q$, as required.

Step 2: $x = \ell$ is a maximum of e(x) on the interval $[\ell, u]$

By Lemma A.1 and the discussion from Step 1, we know that |e(x)| is maximized at q+2 points inside $[\ell,u]$ and q of these points are contained inside the open interval (ℓ,u) . Hence, $x=\ell$ must either be a maximum or a minimum of e(x). We will show that $x=\ell$ must be a maximum by contradiction.

Suppose $x = \ell$ was a minimum of e(x) on $[\ell, u]$. First note that p^* is trivially nonnegative on $[\ell, u]$, or else p(x) = 0 would be a better polynomial. Hence, since $p^*(0) = 0$ we must have $p^{*'}(\delta) > 0$ for some $\delta \in [0, \ell]$, or else the zero polynomial p(x) = 0 would be a better approximation. Hence, for some $\delta \in [0, \ell]$ we have $e'(\delta) < 0$.

We must also have $e'(\ell) \geq 0$ or else $x = \ell$ is not a minimum of e(x). Since $e'(\delta) < 0$ for some $\delta \in [0,\ell]$ and $e'(\ell) \geq 0$, by the intermediate value theorem there exists a point $x^* \in [0,\ell]$ such that $e'(x^*) = 0$. However, by the discussion above we know that all stationary points of e are contained inside the open interval (ℓ,u) . Hence, $x = \ell$ cannot be a minimum of e(x) on $[\ell,u]$. However, by Step 1 we know that the endpoints of $[\ell,u]$ must be either minima or maxima of e(x). Hence, $x = \ell$ is a maximum of e(x) on $[\ell,u]$.

Step 3: Obtaining the desired equalities

Since e(x) has a maximum in $[\ell, u]$ at $x = \ell$, we have $p^*(\ell) = \min_{x \in [\ell, u]} p^*(x)$. The other two equalities are immediate consequences of the equioscillation property of p^* Lemma A.1 and that $x = \ell$ is a minimum of p^* over the set $[\ell, u]$.

With the above-mentioned result in hand, we are ready to prove Theorem 4.1.

Theorem 4.1. Let d be odd and define $\ell_1 = \ell$ and $u_1 = u$. For t = 1, ..., T define

$$p_{t} = \underset{p \in \mathbb{P}_{d}^{\text{odd}}}{\operatorname{argmin}} \max_{x \in [\ell_{t}, u_{t}]} |1 - p(x)|$$

$$\ell_{t+1} = \underset{x \in [\ell_{t}, u_{t}]}{\min} p_{t}(x)$$

$$u_{t+1} = \underset{x \in [\ell_{t}, u_{t}]}{\max} p_{t}(x)$$

$$(9)$$

The resulting composition $p^* := p_T \circ p_{T-1} \circ \cdots \circ p_1$ is optimal and the error is given by:

$$\max_{x \in [\ell, u]} |1 - p^{\star}(x)| = \min_{\substack{p = p_T \circ p_{T-1} \circ \dots \circ p_1 \\ p_t \in \mathbb{P}_d^{\text{odd}}}} \max_{x \in [\ell, u]} |1 - p(x)| = 1 - \ell_{T+1}.$$
 (10)

Furthermore the new error, lower and upper bounds can be computed through

$$\ell_{t+1} = p_t(\ell_t), \quad u_{t+1} = 2 - \ell_{t+1}, \quad \text{and} \quad \max_{x \in [\ell_t, u_t]} |1 - p_t(x)| = 1 - \ell_{t+1}.$$
 (11)

Proof. The proof of (11) is an immediate consequence of Lemma A.2, since for each t = 1, ..., T, p_t is the optimal approximation in $\mathbb{P}_d^{\text{odd}}$ to $x \mapsto 1$.

We now proceed with the proof of (10), which will be by induction. The proof for T=1 is an immediate consequence of Lemma A.2 and we also have $p^*(\ell)=\ell_2$ by (11). Now suppose the result is true for all $t \leq T-1$. For $t=1,\ldots,T-1$, note that the image of p_t on $[\ell_t, u_t]$ is exactly $[\ell_{t+1}, u_{t+1}]$ by i). Hence, if we define $g(x) := p_{T-1} \circ \cdots \circ p_1(x)$, then the image of g on $[\ell, u]$ is $[\ell_T, u_T]$. Furthermore, by i) we also have $g(\ell) = \ell_T$. Pick any f such that $f \neq g$ and

$$f = \widetilde{p}_{T-1} \circ \cdots \circ \widetilde{p}_1,$$

for some $\widetilde{p}_1, \ldots, \widetilde{p}_{T-1} \in \mathbb{P}_d^{\text{odd}}$. Let the image of f on $[\ell, u]$ be [a, b]. We will prove that $\frac{a}{b} \leq \frac{\ell_T}{u_T}$ by contradiction.

Suppose $\frac{a}{b} > \frac{\ell_T}{u_T}$. Define $c = \frac{2}{a+b}$. Then, the image of the scaled function cf on $[\ell, u]$ is [ca, cb] and cf satisfies

$$\max_{x \in [\ell, u]} |1 - cf(x)| = \max \{1 - ca, cb - 1\} = \frac{b - a}{a + b}.$$

Recall by our inductive hypothesis, we have $\max_{x \in [\ell, u]} |1 - g(x)| = 1 - \ell_T = u_T - 1$ where the second equality holds by (11). It follows that

$$\begin{split} \frac{a}{b} > \frac{\ell_T}{u_T} \\ \Leftrightarrow \frac{a}{b} > \frac{\ell_T}{2 - \ell_T} \\ \Leftrightarrow \ell_T < \frac{2a}{a + b} \\ \Leftrightarrow 1 - \ell_T > \frac{b - a}{a + b} \\ \Leftrightarrow \max_{x \in [\ell, u]} |1 - g(x)| > \max_{x \in [\ell, u]} |1 - cf(x)|, \end{split}$$

which leads to a contradiction to our inductive hypothesis that g is optimal. Hence, we must have $\frac{a}{b} \leq \frac{\ell_T}{u_T}$.

Consequently, using that $\frac{a}{b} \leq \frac{\ell_T}{u_T}$, we will show that for any $\widetilde{p}_T \in \mathbb{P}_d^{\text{odd}}$ and for any $f = \widetilde{p}_{T-1} \circ \cdots \circ \widetilde{p}_1$ $\widetilde{p}_T \circ f$ cannot be a better approximation than $p_T \circ g$. In particular, we have

$$\begin{split} \max_{x \in [\ell, u]} |1 - \widetilde{p}_T(f(x))| &\geq \min_{p \in \mathbb{P}_d^*} \max_{x \in [\ell, u]} |1 - p(f(x))| \\ &= \min_{p \in \mathbb{P}_d^*} \max_{x \in [a, b]} |1 - p(x)| \\ &= \min_{p \in \mathbb{P}_d^*} \max_{x \in [a/b, 1]} |1 - p(x)| \\ &\geq \min_{p \in \mathbb{P}_d^*} \max_{x \in [\ell_T/u_T, 1]} |1 - p(x)| \\ &= \min_{p \in \mathbb{P}_d^*} \max_{x \in [\ell_T, u_T]} |1 - p(x)| \\ &= \min_{p \in \mathbb{P}_d^*} \max_{x \in [\ell_T, u_T]} |1 - p(g(x))| \\ &= \max_{x \in [\ell_T, u_T]} |1 - p_T(g(x))| = 1 - p_T(\ell_T) = 1 - \ell_{T+1}, \end{split}$$

where the second and third equality follow by changing variables y = x/b so that

$$\min_{p \in \mathbb{P}^*_d} \max_{x \in [a,b]} |1 - p(x)| = \min_{p \in \mathbb{P}^*_d} \max_{y \in [a/b,1]} |1 - p(by)| = \min_{p \in \mathbb{P}^*_d} \max_{y \in [a/b,1]} |1 - p(y)|$$

and this last equality follows because the space \mathbb{P}_d^* is invariant under input rescaling; that is, for any $b \neq 0$, the map $x \mapsto bx$ preserves the space $\operatorname{span}\{x, x^3, \dots, x^d\}$. This concludes the proof.

B Proof of Theorem 4.3

In this section we provide the proof of the convergence guarantee stated in Theorem 4.3.

Theorem 4.3. Let M be a matrix normalized so that $\sigma(M) \subset [\ell, 1]$. Let $X_T = p^*(M)$, where p^* is the polynomial from Theorem 4.1 with d = 2q + 1. Then, we have

$$\|\operatorname{polar}(\boldsymbol{M}) - \boldsymbol{X}_T\|_2 \le |1 - \ell^2|^{(q+1)^T}.$$
 (13)

Hence, for d=3 the method converges quadratically and for d=5 the method converges cubically.

Proof. Define

$$p^{\star} = \operatorname*{argmin}_{\substack{p = p_T \circ p_{T-1} \circ \cdots \circ p_1 \\ p_t \in \mathbb{P}_d^{\star}}} \max_{x \in [\ell, u]} |1 - p(x)|.$$

Then Algorithm 2 returns $X_T = p^*(M)$. Let $h \in \mathbb{P}_q$ be [q/0] Padé-approximant to $(1-x)^{-1/2}$ [28, Section 3] and define $p(x) = xh(1-x^2) \in \mathbb{P}_d^{\text{odd}}$. Define $f = p \circ \cdots \circ p$ as

the composition of p with itself T times. Then, by Theorem 4.1, [28, Theorem 3.1], and $f(x) \ge 0$ for $x \ge 0$ we have

$$\|\operatorname{sign}(\boldsymbol{M}) - \boldsymbol{X}_T\|_2 \le \max_{x \in [\ell, 1]} |1 - p^*(x)|$$

$$\le \max_{x \in [\ell, 1]} |1 - f(x)|$$

$$\le \max_{x \in [\ell, 1]} \left[\frac{|1 - x^2|^{(d+1)^T}}{1 + f(x)} \right]$$

$$\le |1 - \ell^2|^{(d+1)^T},$$

as required.

C Proof of equivalence between (6) and (7)

In this section we provide a proof for the equivalence between (6) and (7). It is sufficient to show that for any fixed polynomial p we have

$$\varepsilon_1 := \max_{\substack{\boldsymbol{M} \in \mathbb{R}^{m \times n} \\ \sigma(\boldsymbol{M}) \subset [\ell, u]}} \| \operatorname{polar}(\boldsymbol{M}) - p(\boldsymbol{M}) \|_2 = \max_{x \in [\ell, u]} |1 - p(x)| := \varepsilon_2.$$

For any fixed M, by the unitary invariance of the spectral norm we immediately have

$$\left\|\operatorname{polar}(\boldsymbol{M}) - p(\boldsymbol{M})\right\|_{2} = \max_{\sigma_{i} \in \sigma(\boldsymbol{M})} |1 - p(\sigma_{i})| \le \max_{x \in [\ell, u]} |1 - p(x)|.$$

Consequently, $\varepsilon_1 \leq \varepsilon_2$.

Suppose that $x^* \in [\ell, u]$ is chosen so that $|1 - p(x^*)| = \max_{x \in [\ell, u]} |1 - p(x)|$. Without loss of generality, assume $m \ge n$. Letting $\mathbf{M} = x^* \mathbf{U} \mathbf{V}^\mathsf{T}$, for any matrix $\mathbf{U} \in \mathbb{R}^{m \times n}$ and $\mathbf{V} \in \mathbb{R}^{n \times n}$ with orthonormal columns, and noting polar $(\mathbf{M}) = \mathbf{U} \mathbf{V}^\mathsf{T}$ yields

$$\varepsilon_1 \ge \|\operatorname{polar}(\boldsymbol{M}) - p(\boldsymbol{M})\|_2$$

$$= \|\boldsymbol{I}_n - p(x^*)\boldsymbol{I}_n\|_2$$

$$= |1 - p(x^*)|$$

$$= \max_{x \in [\ell, u]} |1 - p(x)| = \varepsilon_2$$

Consequently, $\varepsilon_1 \geq \varepsilon_2$. Hence, $\varepsilon_1 = \varepsilon_2$, as desired.

D Remez algorithm

In this section, we show in detail how to solve (14). By Theorem 4.1, this also gives a solution to (7). We give a closed form solution for d = 3. We then describe how the Remez algorithm [42, 43] can be used to approximate p_t for arbitrary d. We finish with Algorithm 3, a simplified version of Remez for solving (14) with d = 5. Recall (14):

$$\underset{p \in \mathbb{P}_d^{\text{odd}}}{\operatorname{argmin}} \max_{x \in [\ell, u]} |1 - p(x)| \tag{17}$$

We begin with the case when d=3. In this case, there is a simple closed form for the optimal odd polynomial $p^* \in \mathbb{P}_3^{\text{odd}}$ as described in Section 4.2. On a given interval

 $[\ell, u]$, the optimal approximation to the constant function $x \mapsto 1$ is given by the scaled and shifted Newton-Schulz polynomial $p_{NS}(x) = \frac{3}{2}x - \frac{1}{2}x^3$:

$$p^{\star}(x) = \beta p_{\text{NS}}(\alpha x)$$
, where $\alpha = \sqrt{\frac{3}{u^2 + \ell u + \ell^2}}$ and $\beta = \frac{4}{2 + \ell u(\ell + u)\alpha^3}$.

One can verify that this polynomial satisfies the equioscillation condition from Lemma A.1 at $x = \ell, \frac{1}{\alpha}$, u as given in (15), with $\sqrt{-a/(3b)} = 1/\alpha$ and $E = \beta - 1$. Therefore, it must necessarily be the optimal approximation from $\mathbb{P}_3^{\text{odd}}$. Note that when u = 1, the function $x \mapsto p_{\text{NS}}(\alpha x)$ is the same polynomial derived by Chen and Chow [12].

Unfortunately, for larger d, finding closed form expressions for optimal approximations from $\mathbb{P}_d^{\text{odd}}$ becomes challenging, and we know of no closed form solution. However, we can approximate the optimal polynomial using the Remez algorithm. Let d=2q+1. Again recalling Lemma A.1, the optimal polynomial must satisfy the equioscillation property at a set of q+2 points, as in (15). The Remez algorithm finds the equioscillation points $A=\{x_0,\ldots,x_{q+1}\}$ from Lemma A.1 by iteratively refining a sequence of trial points $A^{(k)}=\{x_0^{(k)},\ldots,x_{q+1}^{(k)}\}$ so that $A^{(k)}$ converges to A. From the sequence of trial points $A^{(k)}$ the algorithm also finds a sequence of polynomials $p^{(k)}$ so that $p^{(k)}$ converges to the optimal polynomial. The convergence is very fast, and usually 10 iterations is sufficient to converge to the optimal polynomial up to double precision machine epsilon [42]. More commonly, the Remez algorithm is used to find optimal polynomial approximations to general continuous functions where $d \approx 100$ or even $d \approx 1000$. However, because the polynomial we build to approximate $\operatorname{sign}(x)$ is a composition of polynomials, each of which has a low degree, in our setting the degree d is small, usually d=5. For d=5 the Remez algorithm simplifies significantly. We now describe this simplified algorithm.

We first choose an initial set of trial points $A^{(1)}$, which ideally should come close to satisfying the equioscillation property. From Lemma A.1, the unique optimal approximation $p^* \in \mathbb{P}_5^{\text{odd}}$ satisfies the equioscillation property at four points in $[\ell, u]$. Since the function we wish to approximate is constant, the equioscillation points must be extrema of p^* on $[\ell, u]$. Because p^* is a odd quintic, it can have at most two local extrema on the positive real line, and thus at most two local extrema on $[\ell, u]$. The other two equioscillation points must therefore be the endpoints ℓ and u. Since we know that ℓ and u must be among the true equioscillation points, we always include them in our set of trial points. For notational simplicity, we call the other two points q and r. We initialize $q_1 = \frac{1}{4}\ell + \frac{3}{4}u$ and $r_1 = \frac{3}{4}\ell + \frac{1}{4}u$, since we observe that as $\ell \to u$ these are approximately the other two equioscillation points.

We now show how to refine a candidate set of trial points $A^{(k)} = \{\ell, q_k, r_k, u\}$ to produce $A^{(k+1)} = \{\ell, q_{k+1}, r_{k+1}, u\}$ as well as an approximately equioscillating polynomial p_k . For any fixed set of trial points, we can find a degree-5 odd polynomial $p_k(x) = a_k x + b_k x^3 + c_k x^5$ that satisfies

$$p_k(\ell) = 1 - E_k, \quad p_k(q_k) = 1 + E_k, \quad p_k(r_k) = 1 - E_k, \quad p_k(u) = 1 + E_k$$
 (18)

for some E_k by solving a linear system in a_k, b_k, c_k and E_k . This can be rewritten as follows:

$$\begin{bmatrix} \ell & \ell^3 & \ell^5 & 1 \\ q_k & q_k^3 & q_k^5 & -1 \\ r_k & r_k^3 & r_k^5 & 1 \\ u & u^3 & u^5 & -1 \end{bmatrix} \begin{bmatrix} a_k \\ b_k \\ c_k \\ E_k \end{bmatrix} = \begin{bmatrix} 1 \\ 1 \\ 1 \\ 1 \end{bmatrix}.$$
 (19)

If $A^{(k)}$ were the extrema of the error function $e_k(x) = 1 - p_k(x)$ on $[\ell, u]$, then they would be an equioscillating set for p_k , and p_k would be the solution. Therefore, to refine $A^{(k)}$, we find the extrema of $e_k(x) = 1 - p_k(x)$. These can occur at ℓ , u and the roots of $e'_k(x)$. Setting $e'_k(x) = 0$ yields the quartic equation $5c_kx^4 + 3b_kx^2 + a_k = 0$, whose two solutions are given explicitly by the quadratic formula after the substitution $y = x^2$. We set q_{k+1} and r_{k+1} to be the solutions to this equation and let $A^{(k+1)} = \{\ell, q_{k+1}, r_{k+1}, u\}$. We repeat the procedure until $|E_k| := \max_{x \in [\ell, u]} |1 - p_k(x)| \approx \max_{x \in [\ell, u]} |1 - p_{k+1}(x)| =: |E_{k+1}|$.

We note that the matrix appearing in (19) is a Vandermonde matrix. Vandermonde matrices become notoriously ill-conditioned as the degree grows large [17, Section 4.6]. However, since in our setting we choose d to be small, there is no ill-conditioning due to large degrees. Instead, we observe ill-conditioning when $\ell \approx u$. However, as $\ell/u \to 1$ the optimal polynomial will converge to the polynomial $\frac{x/u}{8} \left(15 - 10(x/u)^2 + 3(x/u)^4\right)$, which can be verified by noting that as $\ell/u \to 1$ all equioscillation points x_0, x_1, x_2, x_3 must converge to u. For general d = 2q + 1, the polynomial will converge to $(x/\ell)h(1 - (x/\ell)^2)$ where $h \in \mathbb{P}_q$ is the [q/0] Padé approximant to $(1-x)^{1/2}$ [28]. In fact, this polynomial is extremely close to the optimal polynomial for sufficiently large ℓ . To see this, let p^* be the optimal approximation from $\mathbb{P}_5^{\text{odd}}$ and let $p(x) = \frac{x/u}{8} \left(15 - 10(x/u)^2 + 3(x/u)^4\right)$. Then,

$$\max_{x \in [\ell, u]} |p^*(x) - p(x)| \le \max_{x \in [\ell, u]} |1 - p(x)| + \max_{x \in [\ell, u]} |1 - p^*(x)|$$
$$\le 2 \max_{x \in [\ell, u]} |1 - p(x)|$$
$$\le 2 (1 - \ell/u)^3.$$

where we invoked [28, Theorem 3.1] and the fact that p^* is the optimal approximation to $x\mapsto 1$ from $\mathbb{P}_5^{\mathrm{odd}}$. Hence, when $\ell/u\geq 1-\epsilon_d^{1/3}$, where $\epsilon_{\mathrm{double}}\approx 1.1\times 10^{-16}$ is the double precision machine epsilon, then $|p^*(x)-p(x)|\leq 2\epsilon_{\mathrm{double}}$. In other words, up to double precision machine epsilon, p^* is equal to p. Therefore, whenever $\ell/u\geq 1-\epsilon_{\mathrm{double}}^{1/3}$ the algorithm simply returns the Padé approximant (that is, the scaled Newton-Schulz polynomial).

The full algorithm is given in Algorithm 3. In our experiments, we never observed Algorithm 3 taking more than five iterations to converge. This algorithm is implemented in full in Appendix G.

E Initialization for Matrices with Large Spectral Gaps

In Section 4, we constructed a sequence of polynomials that is adapted to the range of the singular values $[\ell, u]$. Assuming nothing else about the input, these polynomials are optimal since they provide a good approximation to 1 across the entire interval. However, in many applications, the spectrum has large gaps; that is, there are several large outlying singular values that are well-separated from the rest. For these matrices, it is not necessary for the polynomial to be accurate on the entire interval $[\ell, u]$, only on the range of the small singular values plus a few other isolated points. In this section, we take advantage of this structure to accelerate our method by preprocessing the matrix to eliminate the largest singular values.

The first step is to find small intervals containing each of these large singular values. To find lower bounds, we use subspace iteration, which is a generalization of the power method that approximates multiple singular values simultaneously. Fix k, the number of singular

```
Algorithm 3 Remez algorithm (degree 5 approximation for sign(x))
```

```
input: interval [\ell, u] for u > \ell > 0.

output: Approximation p \in \mathbb{P}_5^{\text{odd}} to p^* = \underset{p \in \mathbb{P}_5^{\text{odd}}}{\operatorname{argmin}} \max_{x \in [\ell, u]} |1 - p(x)|.

define \epsilon_{\text{double}} = 1.11 \times 10^{-16}

if \ell/u \ge 1 - \epsilon_{\text{double}}^{1/3} then

Return p(x) = \frac{x/u}{8} \left(15 - 10(x/u)^2 + 3(x/u)^4\right)

end if

q_1 = \frac{1}{4}\ell + \frac{3}{4}u, \quad r_1 = \frac{3}{4}\ell + \frac{1}{4}u.

E_0 = \infty, \quad E_{-1} = -\infty

k \leftarrow 0

while ||E_k| - |E_{k-1}|| > \epsilon_{\text{double}} do

k \leftarrow k + 1

\begin{bmatrix} a_k \\ b_k \\ c_k \\ E_k \end{bmatrix} = \begin{bmatrix} \ell & \ell^3 & \ell^5 & 1 \\ q_k & q_k^3 & q_k^5 & -1 \\ r_k & r_k^3 & r_1^5 & 1 \\ u & u^3 & u^5 & -1 \end{bmatrix} = \begin{bmatrix} 1 \\ 1 \\ 1 \\ 1 \\ 1 \end{bmatrix}

q_{k+1} = \sqrt{\frac{-3b_k - \sqrt{9b_k^2 - 20a_k c_k}}{10c_k}}, \quad r_{k+1} = \sqrt{\frac{-3b_k + \sqrt{9b_k^2 - 20a_k c_k}}{10c_k}}

end while

Return p(x) = a_k x + b_k x^3 + c_k x^5
```

values we wish to eliminate. Letting $\sigma_1 \geq \cdots \geq \sigma_n$ denote the singular values of M, subspace iteration produces estimates $\tilde{\sigma}_1 \geq \cdots \geq \tilde{\sigma}_k$ satisfying $\sigma_i \geq \tilde{\sigma}_i$ for all $i \in 1, \ldots, k$. To find upper bounds on each σ_i , we can use the fact that $\|M\|_{\mathrm{F}}^2 = \sum_{j=1}^n \sigma_j^2$ as follows:

$$\sigma_i^2 = \|\mathbf{M}\|_{\mathrm{F}}^2 - \sum_{\substack{j=1\\j\neq i}}^n \sigma_j^2 \le \|\mathbf{M}\|_{\mathrm{F}}^2 - \sum_{\substack{j=1\\j\neq i}}^k \sigma_j^2 \le \|\mathbf{M}\|_{\mathrm{F}}^2 - \sum_{\substack{j=1\\j\neq i}}^k \tilde{\sigma}_j^2$$
(20)

That is, for each $i \in [n]$,

$$\sigma_i \in \left[ilde{\sigma}_i, \ \sqrt{\|oldsymbol{M}\|_{ ext{F}}^2 - \sum_{\substack{j=1 \ j
eq i}}^k ilde{\sigma}_j^2}
ight]$$

Setting i = k + 1, the above also provides an upper bound for the tail of the spectrum, $\sigma_{k+1}, \ldots, \sigma_n$.

The second step is to find an odd polynomial that well-approximates the constant function on each of these intervals and on the tail simultaneously. For simplicity, we treat only the k=1 case here. Assume that M is normalized to $\|M\|_{\rm F}=1$ and let $z=\tilde{\sigma}_1$ be the lower bound produced by subspace iteration (which reduces to the power method in this case). Then (20) gives $\sigma_1 \in [z,1]$ and $\sigma_2,\ldots,\sigma_n \leq \sqrt{1-z^2}$. Assume that these intervals do not overlap, that is, $\sqrt{1-z^2} \leq z \Leftrightarrow z \geq 1/\sqrt{2}$. Then we construct the unique

Thet $Q_0 \in \mathbb{R}^{n \times k}$ be a random matrix with orthonormal columns and define $Q_{t+1}, R_{t+1} = \operatorname{qr} \left(M^{\top} M Q_t \right)$, where qr is the QR decomposition. Subspace iteration outputs the singular values $\tilde{\sigma}_1, \ldots, \tilde{\sigma}_k$ of $M Q_T$, $\tilde{\sigma}_1, \ldots, \tilde{\sigma}_k$. By the Cauchy interlacing theorem, $\tilde{\sigma}_k \leq \sigma_k$.

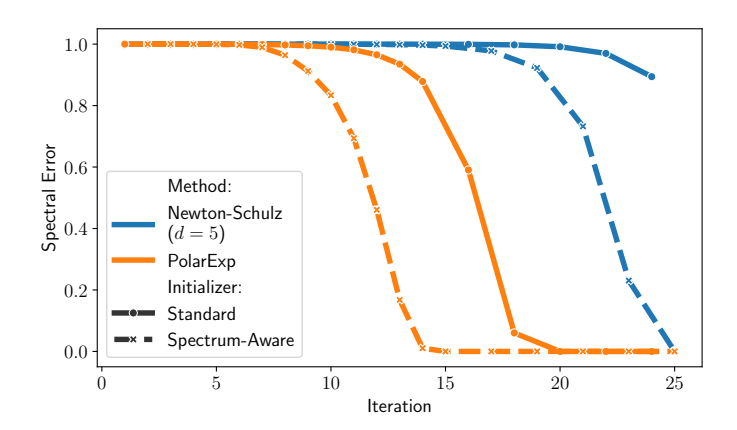


Figure 8: Benefits of the spectrum-aware initialization scheme of Appendix E. Using this scheme improves convergence of both Newton-Schulz and Polar Express on a synthetic 32×32 matrix with $\sigma_j(\mathbf{M}) = j^{-5}$. Note that we count the spectrum-aware initialization as an additional iteration.

odd cubic polynomial $p(x) = ax + bx^3$ that satisfies $p(\sqrt{1-z^2}) = 1$ and p(z) = 1 by setting

$$a = \frac{z^2(z + \sqrt{1 - z^2}) - \sqrt{1 - z^2}}{z\sqrt{1 - z^2}(2z^2 - 1)} \qquad b = \frac{\sqrt{1 - z^2} - z}{z\sqrt{1 - z^2}(2z^2 - 1)}$$
(21)

Because p(0)=0 and p has at most one local extremum on $\mathbb{R}_{\geq 0}$, these conditions immediately guarantee that p is concave-increasing on $[0,\sqrt{1-z^2}]$, so it must lie above the line $x\mapsto x/\sqrt{1-z^2}$. Furthermore, p is decreasing on $[\sigma_1,1]$, so it maps $\sigma_1\in[z,1]$ to [p(1),1]. By minimizing p(1) over all valid z (that is, over the interval $z\in[1/\sqrt{2},1]$), one can further show that $p(1)>1/\sqrt{2}$, so σ_1 cannot be decreased very much by applying p. Thus, the largest singular value of p(M) is still at most 1, while the smaller singular values have increased by a potentially large factor of $1/\sqrt{1-z^2}$. When there is a large outlying singular value, z is close to 1 and this initialization scheme makes much more progress than a standard iteration of PolarExpress would have.

In Figure 8, we demonstrate the benefit of using the p given by (21) on a synthetic matrix whose spectrum follows a power law decay. That is, $\sigma_j(M) = j^{-5}$, so this matrix has a large outlying singular value $\sigma_1 \gg \sigma_2$. Applying (21) costs almost as much as performing an iteration of a degree-5 polynomial method, so for fair comparison, we count it as an additional iteration in this plot. For both Newton-Schulz and Polar Express, performing the extra spectrum-aware initialization step described in this section leads to significant speedups in convergence.

F Fast Polynomial Iteration for Rectangular Matrices

In this section, we describe a simple method for applying an iterative polynomial method to a rectangular matrix. For matrices with a large aspect ratio, this method yields significant computational savings. We emphasize that this method is applicable to any computation of the form $(p_T \circ \cdots \circ p_1)(\mathbf{X})$, where each p_t is an odd polynomial. Thus, it can be used to apply Newton-Schulz or Jordan's polynomials in addition to our own.

As a preliminary, we first describe the baseline approach. Let $X \in \mathbb{R}^{m \times n}$ with $m \ge n$, where $\alpha := m/n \ge 1$ is called the aspect ratio. Any odd polynomial p of degree

d=2q+1 can be represented as $p(x)=xh(x^2)$, where h is a polynomial of degree q. Thus, $p(X) = Xh(X^{\top}X)$. Furthermore, h can be written in a factored form called Horner's rule to reduce the number of multiplications. For instance, if $h(y) = a + by + cy^2 + dy^3$, Horner's rule gives h(y) = a + y (b + y (c + dy)). For a matrix, h(Y) = aI + Y (bI + Y (cI + dY)). Thus for $Y \in \mathbb{R}^{n \times n}$, computing h(Y) costs about $(\deg(h) - 1) \cdot n^3$ operations, and computing $p(X) = Xh(X^{\top}X)$ costs $2mn^2 + \left(\frac{d-1}{2} - 1\right) \cdot n^3 = \left(\frac{d-3}{2} + 2\alpha\right) \cdot n^3$ operations. This process could be repeated for each iteration p_1, \ldots, p_T . Notice that if we instead computed $h(XX^{\top})X$, the result would be the same but the cost would be higher.

A major drawback of this naive approach is that it has a strong dependence on α , since two rectangular matrix multiplications must be performed in each of the T iterations. When $m \gg n$, these two multiplications dominate the cost. In Algorithm 4, we introduce a simple trick that dramatically reduces this cost, using just two rectangular matrix multiplications to compute all T iterations.

Algorithm 4 Fast Polynomial Iteration for Rectangular Matrices

input: $X \in \mathbb{R}^{m \times n}$ with m > 1.5n, odd polynomials $p_1(x) = xh_1(x^2), \dots, p_T(x) = xh_T(x^2)$. **output:** The matrix $(p_T \circ \cdots \circ p_1)(X)$.

$$oldsymbol{Y} = oldsymbol{X}^ op oldsymbol{X}$$
 Let $oldsymbol{Q}_0 = oldsymbol{I}$ for $t = 1, 2, \dots, T$ do $oldsymbol{R}_t = oldsymbol{Q}_{t-1}^ op oldsymbol{Y} oldsymbol{Q}_{t-1}$ by $2n^3$ of $2n^3$ of $2n^3$ denoted for return $oldsymbol{X} oldsymbol{Q}_T$ denoted for $oldsymbol{T}$ and $oldsymbol{T}$ denoted for $oldsymbol{T}$ denote

To see why this works, define $q_0(x) = x$,

$$q_{t}(x) = \frac{(p_{t} \circ \dots \circ p_{1})(x)}{x} = \frac{p_{t}((p_{t-1} \circ \dots \circ p_{1})(x))}{x} = \frac{p_{t}(xq_{t-1}(x))}{x}$$

$$= \frac{xq_{t-1}(x) \cdot h_{t}((xq_{t-1}(x))^{2})}{x} = q_{t-1}(x) \cdot h_{t}(x^{2} \cdot q_{t-1}(x)^{2})$$
(22)

$$= \frac{xq_{t-1}(x) \cdot h_t\left((xq_{t-1}(x))^2\right)}{x} = q_{t-1}(x) \cdot h_t\left(x^2 \cdot q_{t-1}(x)^2\right)$$
(23)

and $r_t(x) = x^2 \cdot q_{t-1}(x)^2$. It is clear by induction that $\mathbf{R}_t = r_t(\mathbf{X}), \mathbf{Q}_t = q_t(\mathbf{X})$, and $\boldsymbol{XQ_T} = (p_t \circ \cdots \circ p_1)(\boldsymbol{X})$. As promised, this algorithm uses no rectangular multiplications in the for-loop. If each p_t is degree d, then the total cost is $\left(\frac{d+3}{2}T+2\alpha\right)\cdot n^3$. When $\alpha > 1.5 \frac{T}{T-1}$, this is smaller than the naive method. We can use this criterion to select either Algorithm 4 or the baseline method at runtime.

Algorithm 4 can introduce numerical errors, especially when working in a low precision format like bfloat16. We identify two sources of numerical trouble and propose remedies for each. The first is due to the ill-conditioning of X. Let $X = U\Sigma V^{\top}$ be the SVD. For large T, $(p_T \circ \cdots p_1)(X) = XQ_T \approx \text{polar}(X) = UV^{\top}$. Thus, $Q_T \approx V^{\top} \Sigma^{-1} V$. When Xhas very small singular values and the floating point precision is very low, instantiating Q_T may be unstable. To mitigate this issue, we use a restarting strategy. Notice that the issue arises only for large T, for which $(p_T \circ \cdots \circ p_1)(\epsilon) \approx 1$. Limiting ourselves to T=3iterations improves the conditioning of Q_T because $(p_T \circ \cdots \circ p_1)(\epsilon) \ll 1$. Thus, to compute T>3 iterations, we begin with X_0 and apply Algorithm 4 with the first three polynomials, producing X_3 . When then apply Algorithm 4 again with the next three polynomials to X_3 , producing X_6 , and so on. As X_t approaches convergence, its conditioning improves

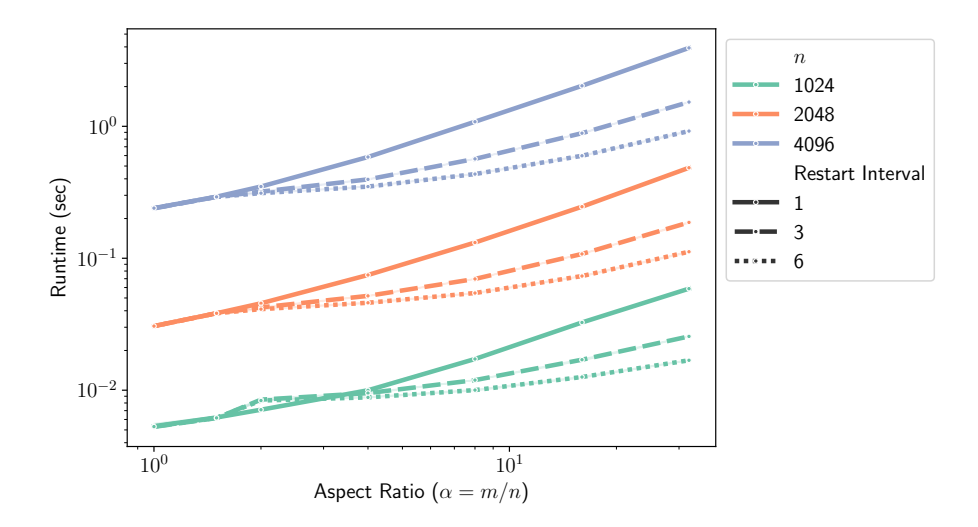


Figure 9: Effects of using Algorithm 4 on runtime on a GPU. We run T=6 iterations of a degree-5 polynomial method on matrices with various dimensions n and aspect ratios α . Restart interval = 6 is Algorithm 4, restart interval = 1 is equivalent to the baseline (that is, not using Algorithm 4), and restart interval = 3 is an intermediate method that calls Algorithm 4 once to do the first three iterations and again to do the last three iterations for greater stability. When $\alpha \gg 1$, increasing the restart interval significantly reduces the runtime.

and we may no longer need to restart at all. Note that restarting Algorithm 4 after every iteration is exactly the same as the baseline method.

Second, while the matrix \boldsymbol{Y} is positive definite in exact arithmetic, numerical round-off can introduce spurious negative eigenvalues that cause the method to diverge to infinity. To combat this issue, we instead set $\boldsymbol{Y} = \boldsymbol{X}^{\top}\boldsymbol{X} + 10^{-3}\boldsymbol{I}$ during the first application of Algorithm 4. (We also normalize by $\|\boldsymbol{X}\|_{\mathrm{F}} + 10^{-3}$ instead of $\|\boldsymbol{X}\|_{\mathrm{F}}$.) In subsequent restarts of Algorithm 4, we set $\boldsymbol{Y} = \boldsymbol{X}^{\top}\boldsymbol{X}$ as before. This is akin to slightly increasing each of the singular values of \boldsymbol{X} , but it does *not* change the polar factor of \boldsymbol{X} . Thus, while the output will be slightly different in the early iterations, the algorithm still converges to the correct answer.

Figure 9 shows that using Algorithm 4 can significantly improve runtime on the GPU when the aspect ratio is large enough. As expected, using Algorithm 4 for many iterations significantly reduces the dependence of the runtime on the aspect ratio. Running six iterations of a degree-5 polynomial method when $\alpha=4$ (as with the linear transformations in each MLP block of a transformer) we obtain almost a 2x speedup, and when $\alpha=32$, we obtain a 5x speedup. If we restart every three iterations, the trend is the same but the runtime savings are somewhat smaller.

F.1 Application to Muon

If these problems can be mitigated, the speed afforded by Algorithm 4 suggests an improvement in the way Muon is applied to transformers. In sum, the idea is to replace one large matrix with a small aspect ratio by many smaller matrices with large aspect ratios and apply Algorithm 4 to all of them in parallel. Each multi-head attention layer contains four square weight matrices W_Q, W_K, W_V and $W_O \in \mathbb{R}^{d \times d}$. The orthogonalization step of

Muon is either applied separately to these four matrices or else to $[\mathbf{W}_Q \mid \mathbf{W}_K \mid \mathbf{W}_V]$ and \mathbf{W}_O , since typical implementations of multi-head attention store the weights in this concatenated form. However, we believe it is natural to consider each of these four weight matrices to be a concatenation of many smaller linear transformations, each corresponding to a single attention head. If H is the number of heads, each of these smaller matrices has size $d \times \frac{d}{H}$; that is, they have aspect ratio $\alpha = H$. The gradient matrices of $[\mathbf{W}_Q \mid \mathbf{W}_K \mid \mathbf{W}_V]$ and \mathbf{W}_O can be reshaped into 3-tensors in which each slice is one of these smaller matrices. Since typical transformers like GPT-3 can have as many as 96 heads, this variation of Muon has the potential to reduce the runtime.

We use this idea to train a GPT-Small model on FineWeb1B. We compare four conditions:

- 1. The baseline approach used in the rest of this paper
- 2. Splitting up the gradient matrices of $[W_Q \mid W_K \mid W_V]$ and W_O by head and applying Muon to each piece, as described above
- 3. Using Algorithm 4, restarted after three iterations
- 4. Splitting by head and using Algorithm 4

We used Polar Express with weight decay of 0.1 for all conditions and swept learning rates 0.003, 0.005, 0.01. Otherwise, all hyperparameters were the same as in Section 5.2.

Our results showed that these changes had a negligible effect in this setting. They did not affect the optimization quality. Compared to the baseline, splitting by heads actually reduced the final loss slightly from 3.59 to 3.55; using Algorithm 4 increased the loss very slightly, from 3.59 to 3.60 when not splitting by head, and from 3.55 to 3.56 when we did split. However, the runtimes of all 12 runs were nearly identical, showing that at this scale, the FLOP savings of Algorithm 4 is not beneficial. The embedding size of GPT-Small is just 768. These techniques may be more impactful when using a larger model. It may also have more impact outside of deep learning, where Polar Express would be run for more than the 5 iterations used in our experiments. We leave exploration of these settings to future work.

G Code for Constructing Polynomials of Polar Express

The following code gives a Python implementation of the offline stage of Algorithm 2. This code was used to construct the coefficients of the polynomials given in (1), which in turn were used in our Muon experiments (Section 5.2). It uses $\ell = 10^{-3}$ and u = 1 by default. It incorporates Algorithm 3 and the finite precision considerations described in Section 4.4.

```
from math import inf, sqrt
import numpy as np

def optimal_quintic(l, u):
    assert 0 <= 1 <= u
    if 1 - 5e-6 <= 1 / u:
        # Above this threshold, the equioscillating polynomials
        # is numerically equal to...
        return (15/8)/u, (-10/8)/(u**3), (3/8)/(u**5)
# This initialization becomes exact as 1 -> u
```

```
q = (3*1 + 1) / 4
   r = (1 + 3) / 4
    E, old_E = inf, None
    while not old_E or abs(old_E - E) > 1e-15:
        old_E = E
       LHS = np.array([
            [1, 1**3, 1**5, 1],
            [q, q**3, q**5, -1],
            [r, r**3, r**5, 1],
            [u, u**3, u**5, -1],
        ])
        a, b, c, E = np.linalg.solve(LHS, np.ones(4))
        q, r = np.sqrt((-3*b + np.array([-1, 1]) *
                        sqrt(9*b**2 - 20*a*c)) / (10*c))
    return float(a), float(b), float(c)
def optimal_composition(1, num_iters, cushion=0.02407327424182761):
    u = 1
    coefficients = []
    for _ in range(num_iters):
        a, b, c = optimal_quintic(max(1, cushion*u), u)
        # Due to cushioning, this may be centered around 1 with
        # respect to 0.024*u, u. Recenter it around 1 with respect
        # to 1, u, meaning find c so that 1 - c*p(1) = c*p(u) - 1:
       pl = a*l + b*l**3 + c*l**5
       pu = a*u + b*u**3 + c*u**5
       rescalar = 2/(pl + pu)
       a *= rescalar; b *= rescalar; c *= rescalar
        # Optionally incorporate safety factor here:
        # a /= 1.01; b /= 1.01**3; c /= 1.01**5
        coefficients.append((a, b, c))
       1 = a*1 + b*1**3 + c*1**5
       u = 2 - 1
    return coefficients
print(*optimal_composition(1e-3, 10), sep="\n")
```